Settling Control Schemes for Dual Actuator Systems for Hard Disk Drives

Jiagen Ding and Masayoshi Tomizuka
Department of Mechanical Engineering
University of California at Berkeley, Berkeley, CA 94720-1740

Abstract

The dual actuator system consists of a coarse actuator(voice coil motor) and a fine actuator (peizoelectric transducer, PZT). This report discusses two design methods for settling controllers for dual actuator systems for hard disk drives. One method is the dual actuator reference trajectory re-design(RTRD) method and the other is the dual actuator initial value compensation(IVC) method. In the RTRD method, the design is divided into three steps. In the first step, the coarse actuator loop is designed to be stable and achieve the basic performance. In the second step, the fine actuator path is designed by loop shaping for superior performance of the overall system. Finally the reference signals are generated for both VCM and PZT actuators. The RTRD method is first presented as a single rate scheme, and the incorporation of dual rate sampling to RTRD is described. In the dual rate RTRD scheme, the coarse actuator works at slow sampling frequency and the fine actuator works at fast sampling frequency. In the IVC method, non-zero initial values are assigned to both VCM and PZT controller states when servo control switches from track seeking to track following, so that the initial state of the plant does not cause any residual vibration. The proposed design methods are evaluated by simulations.

October 2001

1 Introduction

The hard disk drive industry continues to strive for increased areal storage densities and reduced data access times. This necessiates performance improvements of the head positioning system in terms of fast transition from one track to another (track seeking), fast and accurate settling(track settling), and precise track following of the target track(track following). To achieve these improvements, the servo bandwidth of the head positioning system must be increased to lower the sensitivity to disturbances such as disk flutter vibrations, spindle motor run-out, windage, and external vibration.The servo bandwith, however, is mainly limited by the mechanical resonance of the head positioning system. Dual-actuator systems offer one way to enlarge the servo bandwidth. The dual-actuator disk file system consists of two actuators: coarse and fine actuators. The coarse actuator is low bandwidth but has a large stroke; the voice coil motor (VCM) is the most popular coarse actuator. The fine actuator is high bandwidth but has a small stroke; The piezoelectric transducer(PZT) is a popular fine actuator. Many research groups have proposed and manufactured dual actuator prototypes. Research efforts have also been devoted to design a simple and high performance dual-actuator servo system [2, 3, 4, 5, 6].

In dual-actuator servo systems, the VCM actuator output and PZT actuator output are not measured separately, but usually only the total sum of the two actuator outputs is available to the servo controller. Namely, the dual actuator system is a DISO(dual-input/single output) system and the servo controller is a SIDO(single input/dual output) system. The controller design is a special case of multi-input/multi-output system (MIMO) design. MIMO design techniques such as LQG [7], H_∞ and $\mu-$synthesis [8] have been applied to the design of dual-actuator disk drive systems. These techniques usually result in high order controllers even after model reduction, which are hard to implement on actual hardware.

The PQ method [15] reduces the MIMO design to two SISO design problems in the frequency domain. The PQ method, however, does not guarantee the stability of the VCM

feedback loop. The VCM feedback loop should be stable so that the disk drive still works safely when the PZT actuator is not activated. Short-span track seeking has been proposed for a dual-actuator system in [17]. The PZT actuator will be first driven to its saturation limit when the track seeking distance is larger than $1\mu m$ [17] , which is not desired for the PZT actuator. The reference trajectory re-design(RTRD) method was first introduced to dual actuator systems by Numasato and Tomizuka in [18]. in [18], the trajectory re-design was performed only for the VCM actuator. Initial value compensation is discussed for single actuator servo systems in [19, 20].

This report extends the work of Numasato and Tomizuka[18] on the RTRD for the dual-actuator system. Settling control is intended to provide smooth transitions from track seeking control to track following control and the objectives of the settling controller are to decrease the settling period and to minimize residual vibrations. The design of RTRD system is divided into three steps: 1) the VCM feedback loop is first designed to be stable, 2) the PZT path is designed to improve the system performance, and 3) the reference trajectories are designed for the VCM and PZT actuators. The bandwidth of the PZT loop will be naturally set higher than that of the VCM loop. This leads us to consider dual rate RTRD control: a fast sampling rate for the PZT path and a slow sampling rate for VCM. This approach achieves smoother settling. The IVC settling control is discussed for track following controllers configured in the parallel structure or decoupled structure for the two actuators[18].

The remainder of this report is organized as follows. Section 2 presents the sturcture and modeling of the dual-actuator system. Section 3 reviews the mode switching control for hard disk drive systems. Section 4 discusses the RTRD design for the dual-actuator system. Section 5 presents the IVC settling control for the parallel and decoupled track following controllers. Section 6 demonstrates a design example for the two settling methods. Section 7 presents the simulation results for the RTRD settling and the IVC settling method. Concluding remarks are given in section 8.

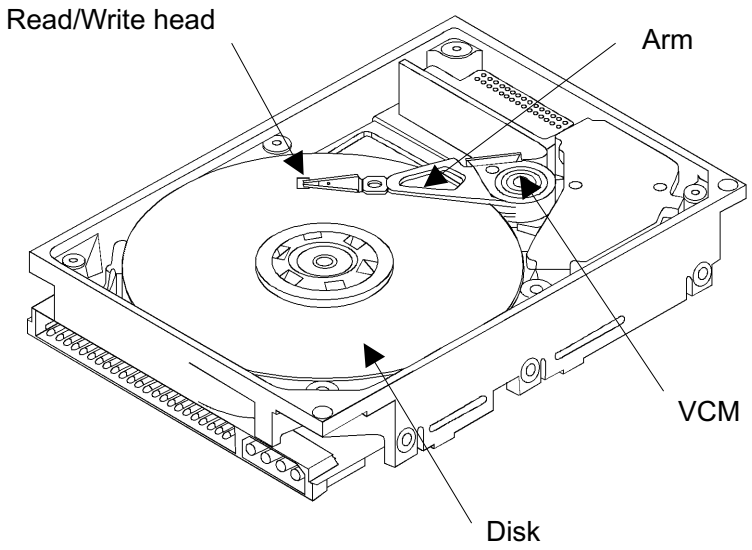

Figure 1: Schematic Diagram of Hard Disk Drive

2 Dual-Actuator System Model

Figure 1 shows the schematic of a hard disk drive system. In this work, we consider a dual actuator system consisting of a voice coil actuator(VCM) as a coarse actuator and a piezoelectric actuator(PZT) as a fine actuator (Fig. 2). The VCM is a conventional actuator used for commercial hard disk drive systems. The fine actuator is an active suspension, which finely moves the Read/Write(R/W) head laterally. The fine actuator(Fig.3) is located between the head suspension and the base plate, which is moved by VCM. A slider is attached to the tip of the suspension. The advantage of this moving suspension type actuator is that it does not require substantial modifications to the shape of the head suspension assembly. However, the servo bandwidth of a prototype dual actuator system by Hitachi[17] is limited to about 3KHz because of the primary resonance mode of the suspension.

2.1 PZT actuator

The fine actuator is placed at the carriage end of the suspension load beam(see Fig. 3). It has two piezoelectric elements which are in parallel. The two piezoelectric elements are oppositely polarized so that one expands and the other contracts when the same voltage

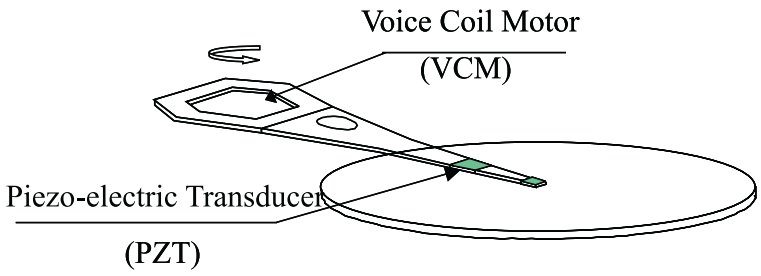

Figure 2: Dual Actuation with Voice Coil Motor and Piezoelectric Transducer

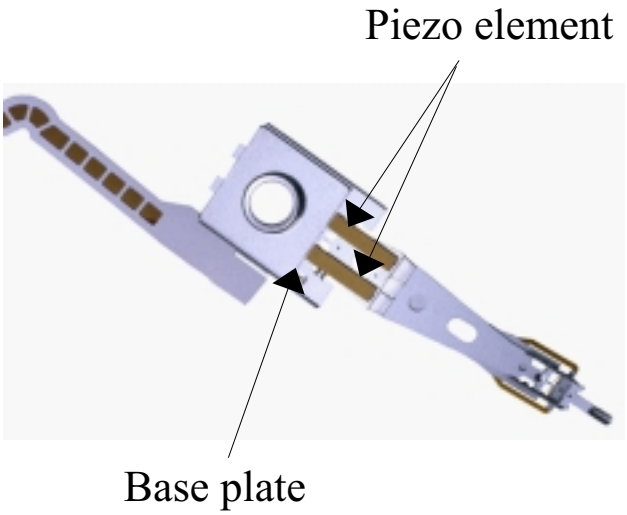

Figure 3: Piezo-electric Transducer(PZT)

potential is applied to them. This results in rotation of the load beam and off track motion of a slider. The driving voltage is applied to the top surface of piezoelectric elements, and the suspension serves as the ground return path(Figure3). Typical piezoelectric actuators attain a stroke displacement of about 2 μm.

2.2 Dual Actuator Transfer Function

The coarse actuator is a conventional Voice Coil Motor(VCM). Since the inertia and force of PZT are much smaller than those of VCM, and the PZT exhibits the first resonant frequency at $8.2kHz$(Hitachi PZT), which is significantly higher than the bandwidth of VCM , the dual actuator system model is decoupled into the VCM transfer function P_{VCM} and the PZT transfer function P_{PZT} generating the relative displacement of R/W head. The VCM is

modeled as a second order system, the transfer function of which looks like a double integrator at relatively high frequencies but flattens out at low frequencies due to pivot bearing friction effect. High resonant mode is also included in the VCM model. The PZT actuator(including the analog notch filter) is modeled as a second order system with the resonance frequency at $8.2kHz$. Computational delay is represented by a first order Pade approximation for each of the two actuators. The transfer function models of the two actuators are:

$$P_{VCM}(s) = K_{vcm}\frac{\omega_1^2}{s^2 + 2\zeta_1\omega_1 s + \omega_1^2}\frac{\omega_2^2}{s^2 + 2\zeta_2\omega_2 s + \omega_2^2}\frac{-0.5D_1 s + 1}{0.5D_1 s + 1} \tag{1}$$

$$P_{PZT}(s) = K_{pzt}\frac{\omega_3^2}{s^2 + 2\zeta_3\omega_3 s + \omega_3^2}\frac{-0.5D_2 s + 1}{0.5D_2 s + 1} \tag{2}$$

In this work, the model parameters for track following control are given in the following two tables:

Table 1: VCM Parameters

Item	K_{vcm}	D_1	ω_1	ζ_1	ω_2	ζ_2
VCM	$2.263e-3$	$44\mu s$	$2\pi * 100$	0.2	$2\pi * 3100$	0.070

Table 2: PZT Parameters

Item	K_{pzt}	D_2	ω_3	ζ_3
PZT	$3.17e-7$	$8.6\mu s$	$2\pi * 8200$	0.4

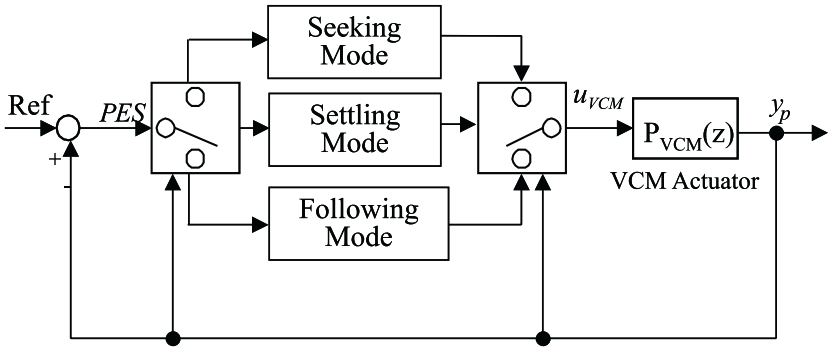

Figure 4: Mode Switching Control System

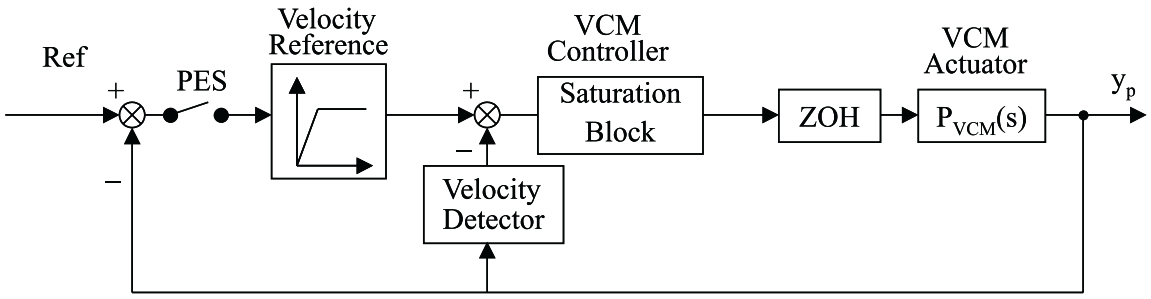

Figure 5: Proximate Time Optimal(PTO) System

3 Mode-Switching Control

The disk servo controller has two main functions. The first is to precisely position the read-write head on a desired track, which is the track following function. The second is to move the head to a target track for retrieving or recording data as quickly as possible, which is the track seeking function. The conventional servo control method for providing the two functions is mode switching control(MSC)[19]. Figure 4 shows the schematic diagram of MSC for hard disk drives. The controllers are selected in the sequence of the seeking controller, the settling controller, and the following controller. Seeking controller is designed for fast motion from one track to another; the settling controller is designed for fast and accurate settling, and the following controller is designed for precise following of the target track. A typical seeking controller is given in Fig. 5, which is a proximate time optimal (PTO) controller based on velocity feedback[11]. The track following controller can be designed via lead-lag

based manual loop shaping or advanced design techniques such as H_∞ design.

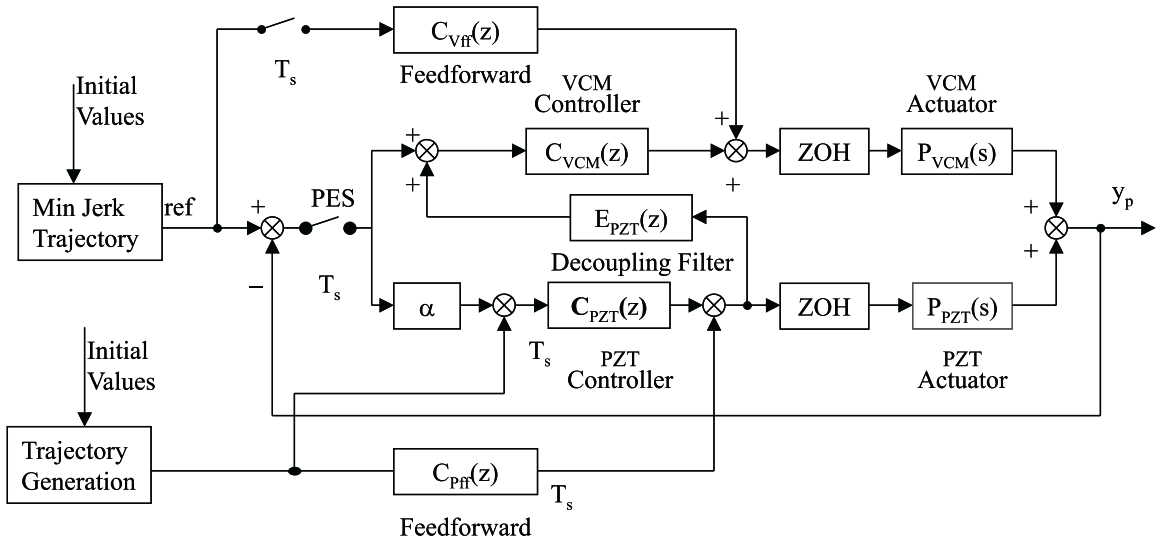

Figure 6: Decoupled Track Following Control

4 RTRD Settling Control for HDD

4.1 Overall Structure of HDD Servo System during Settling Mode

Figure 6 shows the overall structure of HDD servo system during settling. It consists of the track following or regulation controller, the feedforward controller and the reference trajectory generator for each of the two actuators, VCM and PZT. In the figure, $P_{VCM}(s)$ and $P_{PZT}(s)$ represent the dynamics of VCM and PZT, respectively. The feedback controllers for VCM and PZT are represented by $C_{VCM}(z)$ and $C_{PZT}(z)$, and the feedforward controller by $C_{Vff}(z)$ and $C_{Pff}(z)$. $E_{PZT}(z)$ is called the decoupling filter. It is an extension of the structure proposed by Numasato and Tomizuka[18]. The new element in Fig.6 are the feedforward controller and the trajectory generator for PZT. We notice the following features about the proposed structure.

(1)In the regulation loop, the VCM and PZT paths would be parallel if the decoupling filter were zero. In this case, both the VCM controller and the PZT controller in the feed back loop respond to the position error signal(PES), which introduces dyanmic coupling between the two actuators. If the decoupling filter closely approximates the dynamics of the PZT actuator, the output of the decoupling filter fed back to the VCM controller with a positive

sign will cancel the output of the PZT actuator fed back to the VCM controller via the PES feedback signal. The cancellation implies that the VCM controller does not see the PZT loop, and in this sense the VCM loop is decoupled from the PZT loop. For this reason, $E_{PZT}(z)$ is called the decoupling filter.

(2)The overall structure during settling is a two-degree-of-freedom structure. As shown in the figure, both the VCM and PZT actuators recieve inputs from the feedback controller and feedforward controller.

(3)The variable gain α in the PZT path allows to "softly" switch on the PZT(feedback) controller for smooth settling. It may be gradually increased from 0 to 1[18]. The effect of α will be shown later in the section on simulations.

(4)The inputs to the feedforward controllers, reference trajectories, are re-designed in real time as the R/W head approaches the target track. The trajectories are re-designed as fucntions of the current VCM's state, which includes the position, velocity and acceleration. For this reason, the proposed mehtod is called the reference trajectory re-design(RTRD) method. The design of reference trajectories will be in 4.2.

4.1.1 VCM Controller Design

To guarantee the stability of the dual-actuator system even in the case that the PZT actuator is not activated, the VCM feedback loop should be stable by itself. In the first step, the VCM controller $C_{VCM}(z)$ is designed so that the VCM feedback loop has basic performance and appropriate stability.

In the design of the feedback controller for the VCM actuator, the sensitivity of the VCM $S_{VCM}(z)$ is used as the performance index and the gain and phase margins of the VCM actuator open loop transfer function $L_{VCM}(z)$ are used for stability evaluation.

$$S_{VCM}(z) = \frac{1}{1 + C_{VCM}(z)P_{VCM}(z)} \tag{3}$$

$$L_{VCM}(z) = C_{VCM}(z)P_{VCM}(z) \tag{4}$$

In the decoupled controller structure, if the PZT actuator is not switched on, the VCM actuator output y_{VCM} is related to the VCM position reference signal r_{VCM} via:

$$y_{VCM} = \frac{C_{Vff}(z)P_{VCM}(z) + C_{VCM}(z)P_{VCM}(z)}{1 + C_{VCM}(z)P_{VCM}(z)} r_{VCM} \tag{5}$$

If $C_{Vff}(z)P_{VCM}(z) \approx 1$, then $y_{VCM} \approx r_{VCM}$. In the settling controller design, the VCM actuator model is approximately a double integrator, so that the feedforwad signal for the VCM actuator may be the acceleration reference signal, i.e. the second derivative of r_{VCM}, instead of r_{VCM} and $C_{Vff}(z)$ may be reduced to a constant, i.e. the mass of the VCM actuator.

4.1.2 PZT Controller Design

In this step, the PZT controller $C_{PZT}(z)$ and a decoupling filter $E_{PZT}(z)$ are designed in order to achieve superior performance of the dual-actuator system. The decoupling filter $E_{PZT}(z)$ is an open loop estimator of the PZT actuator output. The total loop sensitivity function and total open loop transfer function are:

$$S_D(z) = \frac{1}{1 + C_{VCM}(z)P_{VCM}(z) + C_{PZT}(z)P_{PZT}(z) + C_{PZT}(z)E_{PZT}(z)C_{VCM}(z)P_{PZT}(z)} \tag{6}$$

$$L_D(z) = C_{VCM}(z)P_{VCM}(z) + C_{PZT}(z)P_{PZT}(z) + C_{PZT}(z)E_{PZT}(z)C_{VCM}(z)P_{PZT}(z) \tag{7}$$

If $E_{PZT}(z) = P_{PZT}(z)$, the total loop sensitivity function can be written as:

$$S_D(z) = \frac{1}{(1 + C_{VCM}(z)P_{VCM}(z))(1 + C_{PZT}(z)P_{PZT}(z))} \tag{8}$$

Let the PZT loop sensitivity function be:

$$S_{PZT}(z) = \frac{1}{1 + C_{PZT}(z)P_{PZT}(z)} \tag{9}$$

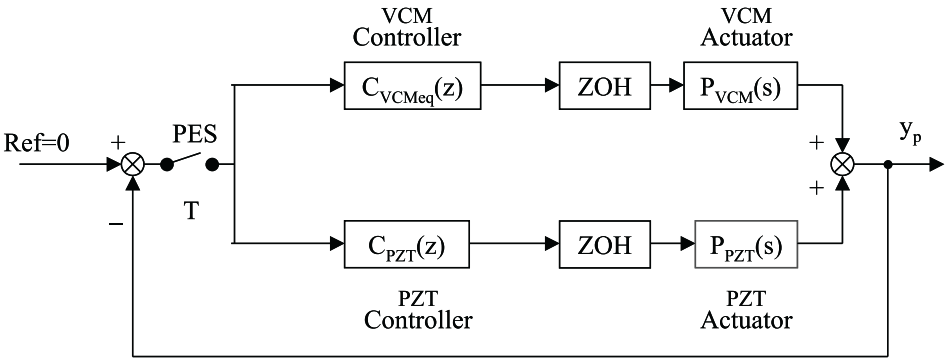

Figure 7: Equivalent Parallel Control Structure

The total sensitivity fucntion is the product of the VCM loop sensitivity function and the PZT loop sensitivity function. The performance index for PZT feedback controller design is the overall loop sensitivity function $S_D(z)$. Since the two actuators are decoupled, the design is reduced to shape the PZT loop sensitivity fucntion to ensure that the total sensitivity function $S_D(z)$ satisfies the performance requirement. The gain and phase margins of the overall open loop transfer function $L_D(z)$ are used as the stability measures.

The decoupled control structure can be considered as an equivalent parallel control structure in Fig. 7. The equivalent VCM controller is

$$C_{VCMeq}(z) = (1 + C_{PZT}(z)E_{PZT}(z))C_{VCM}(z) \tag{10}$$

Other indexes that should be considered in the PZT feedback controller design are the relative gain and phase between the equivalent VCM path and the PZT path[21]:

$$R(z) = \frac{C_{VCMeq}(z)P_{VCM}(z)}{C_{PZT}(z)P_{PZT}(z)} \tag{11}$$

Because of the low bandwidth nature of the VCM actuator $P_{VCM}(z)$ and the high bandwidth but small stroke nature of the PZT actuator $P_{PZT}(z)$, $C_{VCMeq}(z)P_{VCM}(z)$ should be large at low frequencies and $C_{PZT}(z)P_{PZT}(z)$ should be large at high frequencies. When the magnitude of $R(z)$ is close to 1, the phase should be far from ± 180 degrees; otherwise the two actuators will fight each other resulting in ineffective control. Actually, for the two actuators

to work together, the phase difference between the two paths must be within ±120 degrees at the frequency where the two paths have an identical gain.

The position outputs $y_{pV}$and y_{pP} due to VCM and PZT reference inputs r_{VCM} and r_{PZT} are respectively:

$$y_{pV} = \frac{C_{Vff}(z)P_{VCM}(z) + C_{PZT}(z)P_{PZT}(z) + (1 + C_{PZT}(z)E_{PZT}(z))C_{VCM}(z)P_{VCM}(z)}{1 + C_{PZT}(z)P_{PZT}(z) + (1 + C_{PZT}(z)E_{PZT}(z))C_{VCM}(z)P_{VCM}(z)} r_{VCM} \tag{12}$$

$$y_{pP} = \frac{C_{Pff}(z)P_{PZT}(z) + C_{PZT}(z)P_{PZT}(z) + (C_{PZT}(z) + C_{Pff}(z))E_{PZT}(z)C_{VCM}(z)P_{VCM}(z)}{1 + C_{PZT}(z)P_{PZT}(z) + (1 + C_{PZT}(z)E_{PZT}(z))C_{VCM}(z)P_{VCM}(z)} r_{PZT} \tag{13}$$

If the PZT estimator is $E_{PZT}(z) = P_{PZT}(z)$, the VCM actuator feedforward controller is $C_{Vff}(z) \approx P_{VCM}^{-1}(z)$ and the PZT actuator feedforward controller is $C_{Pff}(z) \approx P_{PZT}^{-1}(z)$, then the above two equations may be reduced to:

$$y_{pV} \approx r_{VCM},\ y_{pP} \approx r_{PZT} \tag{14}$$

The overall R/W head poisition y_p is the sum of $y_{pV}$and y_{pP}. Because of Eq. 14, the VCM and PZT actuator reference signals should be designed such that their sum is the desired reference.

4.2 Reference Trajectory Re-design

The settling control objectives are achieved by computing the reference signals for the VCM and PZT actuators T_f seconds ahead of the expected completion time of settling, such that the overal position y_p due to the states of VCM actuator at the switching instant(position, velociy and acceleration) may be brought to zero at the expected instant of seek completion. The VCM actuator trajectory is generated by minimizing the jerk[18] during the transition and the PZT actuator trajectory is introduced for further shortening the settling time.

The minimum jerk VCM trajectory $r_{VCM}(t)$ with nonzero initial acceleration a_0,velociy v_0 and position p_0 is generated by minimizing the objective function,

$$\int_0^{T_f} (\frac{d^3 r_{VCM}(t)}{dt^3})^2 dt \tag{15}$$

subject to

$$r_{VCM}(0) = p_0, r'_{VCM}(0) = v_0, r''_{VCM}(0) = a_0 \tag{16}$$

Solving this minimization problem by the Lagrange multiplier method, the position and acceleration trajectory signals are:

$$\begin{aligned} r_{VCM}(t) &= \frac{T_f^2}{2}[-(\frac{t}{T_f})^5 + 3(\frac{t}{T_f})^4 - 3(\frac{t}{T_f})^3 + (\frac{t}{T_f})^2]a_0 \\ &+ T_f[-3(\frac{t}{T_f})^5 + 8(\frac{t}{T_f})^4 - 6(\frac{t}{T_f})^3 + (\frac{t}{T_f})^2]v_0 \\ &+ [-6(\frac{t}{T_f})^5 + 15(\frac{t}{T_f})^4 - 10(\frac{t}{T_f})^3 + 1]p_0 \end{aligned} \tag{17}$$

$$\begin{aligned} r''_{VCM}(t) &= [-10(\frac{t}{T_f})^3 + 18(\frac{t}{T_f})^2 - 9(\frac{t}{T_f}) + 1]a_0 \\ &+ \frac{4}{T_f}[-15(\frac{t}{T_f})^3 + 24(\frac{t}{T_f})^2 - 9(\frac{t}{T_f})]v_0 \\ &+ \frac{60}{T_f^2}[-2(\frac{t}{T_f})^3 + 3(\frac{t}{T_f})^2 - (\frac{t}{T_f})]p_0 \end{aligned} \tag{18}$$

Rewrite the minimum jerk position reference signal as

$$r_{VCM}(t) = F_a(t, T_f)a_0 + F_v(t, T_f)v_0 + F_p(t, T_f)p_0 \tag{19}$$

where T_f is the settling time, the $F_a(t, T_f)$,$F_v(t, T_f)$ and $F_p(t, T_f)$ are given by

$$\begin{aligned} F_a(t, T_f) &= \frac{T_f^2}{2}[-(\frac{t}{T_f})^5 + 3(\frac{t}{T_f})^4 - 3(\frac{t}{T_f})^3 + (\frac{t}{T_f})^2] \\ F_v(t, T_f) &= T_f[-3(\frac{t}{T_f})^5 + 8(\frac{t}{T_f})^4 - 6(\frac{t}{T_f})^3 + (\frac{t}{T_f})^2] \\ F_p(t, T_f) &= -6(\frac{t}{T_f})^5 + 15(\frac{t}{T_f})^4 - 10(\frac{t}{T_f})^3 + 1 \end{aligned} \tag{20}$$

and may be computed offline.

When there is no PZT reference trajectory(zero reference for PZT), the R/W head will follow the VCM reference trajectory $r_{VCM}(t)$ and arrive at the target track at time T_f. If the PZT trajectory $r_{PZT}(t)$ is introduced, the R/W head will follow the trajectory $r_{VCM}(t) + r_{PZT}(t)$, the head trajectory $r_H(t)$. If this head trajectory $r_H(t)$(Eq.21) is also a minimum jerk trajectory generated for the same VCM intial states as for $r_{VCM}(t)$ but with a shorter settling time T_H, the R/W head will follow this minimum jerk head trajectory $r_H(t)$ and arrive at the target track at time T_H, which is sooner than T_f.

$$r_H(t) = F_a(t, T_H)a_0 + F_v(t, T_H)v_0 + F_p(t, T_H)p_0 \tag{21}$$

The PZT reference trajectory is obtained by subtracting $r_{VCM}(t)$ from $r_H(t)$

$$\begin{aligned} r_{PZT}(t) &= r_H(t) - r_{VCM}(t) \\ &= (F_a(t, T_H) - F_a(t, T_f))a_0 + (F_v(t, T_H) - F_v(t, T_f))v_0 + (F_p(t, T_H) - F_p(t, T_f))p_0 \end{aligned}$$

Since $r_H(t)$ and $r_{VCM}(t)$ are both minimum jerk trajectories, $r_H(t)$ and r_{VCM} will be smooth signals, then the PZT reference trajectory will also be smooth. This determination of $r_{PZT}(t)$ makes sense because PZT has a higher bandwidth than VCM.

4.3 Soft Switching and Stability of the Closed Loop System

A time-varying parameter $\alpha(t)$ is introduced in front of the PZT feedback controller to achieve soft switching of the PZT feedback controller. $\alpha(t)$ is gradually increased from 0 to 1 for avoiding the saturation of the PZT actuator and excitation of the unmodeled dynamcis of the two actuators. While this soft switching scheme is practical, the overall system becomes time varying and it is important to assure that the system remains stable.

Stability is discussed for a pratical case where α is switched N times from 0, α_1, α_2..., to α_N sequentially, while it is fixed during each of time intervals $[0, t_1]$,$[t_1, t_2]$,...and $[t_{N-1}, t_N]$. In each time interval, α is a constant and the dual actuator system is a linear system $L_{\alpha_i}(\alpha_i, i =$

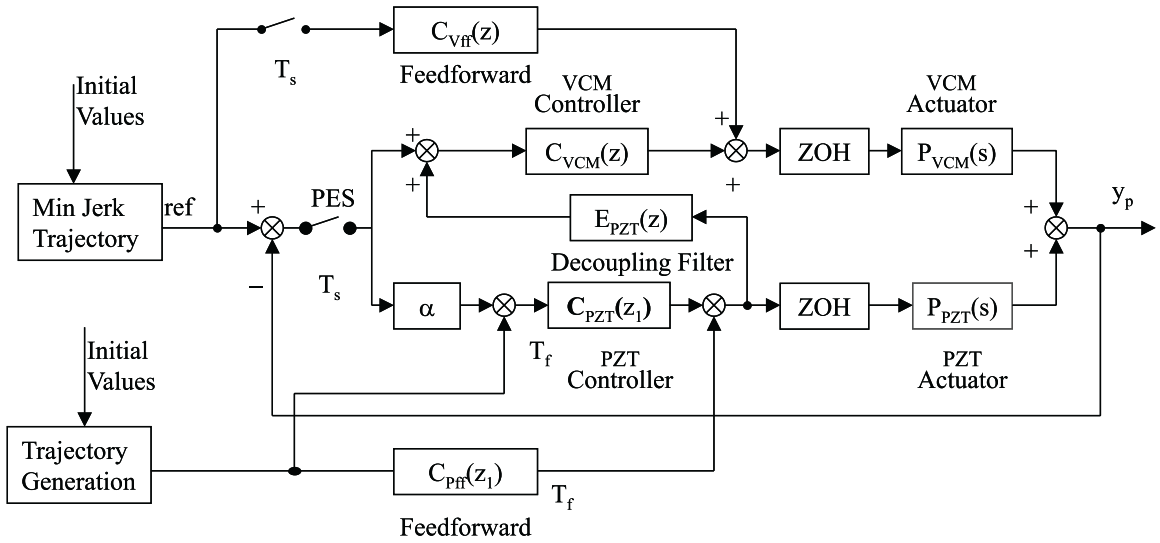

Figure 8: Dual-rate Dual Actuator Servo System for RTRD Settling Control

$1...N$). Given the initial state $\mathbf{x_0}$ of the overall system, the system states $\mathbf{x}_t$ at any time $t(t \in [t_j, t_{j+1}], j = 0, ..N, t_0 = 0, t_{N+1} = \infty)$ may be obtained as follows:

$$\begin{aligned} \mathbf{x}_1 &= L_{\alpha_1}(t_1, \mathbf{x}_0) \\ \mathbf{x}_2 &= L_{\alpha_2}(t_2 - t_1, \mathbf{x}_1) \\ &\ldots \\ \mathbf{x}_t &= L_{\alpha_j}(t - t_j, \mathbf{x}_j) \end{aligned} \tag{22}$$

where $L_{\alpha_i}(t, \mathbf{x}_i)$ denotes the response of the linear system L_{α_i} at time t with initial state $\mathbf{x}_i$ at $t = t_i$. Since there is only a finite number of switchings(N is finite) and L_{α_N}, which corresponds to $\alpha = 1$, is asymptotically stable, the stability is garanteed for the dual actuator system. In practice, all L_{α_i}'s$(i = 1, ...N)$ are expected to be stable.

4.4 Dual Rate Control for RTRD Settling Control

In this section, we explore the possibility of dual rate control for the RTRD scheme for the dual actuator system. Dual rate control is a special kind of multirate control. Multirate control has been applied to the traditional single actuator hard disk drive to achieve better acoustics during seek [9]. Multirate state estimator scheme has been applied to hard disk

drives for achieving smooth control input update[10]. In the dual rate controller design discussed in [11], the fast sampling controller is first designed, and then the slow sampling controller is designed. In case of the RTRD settling scheme, however, the VCM path was designed first, and the PZT path was designed for improved performance. Since the PZT loop has a higher bandwidth than the VCM loop, it makes sense to apply higher sampling rate to the PZT loop. This implies that the slow sampling controller is designed first, and then the fast sampling controller is designed.

Figure 8 shows the dual-rate dual-actuator servo system for RTRD settling control. The digital dual rate dual-actuator servo system is working at two sampling frequencies. The VCM feedforward controller $C_{Vff}(z)$ and feedback controller $C_{VCM}(z)$ are updated at slow sampling frequency($\frac{1}{T_s}$). The feedforward controller $C_{Pff}(z_1)$ and feedback controller $C_{PZT}(z_1)$ of the PZT actuator are updated at high sampling frequency($\frac{1}{T_f}$), which achieves smoother settling. Note that z and z_1 in Fig. 8 correspond to the slow and fast sampling rates, respectively.

The feedforward and feedback controllers($C_{Vff}(z)$ and $C_{VCM}(z)$) for the VCM actuator are designed and implemented as in the single rate case. On the other hand, the feedback controller $C_{PZT}(z_1)$ for the PZT actuator at high sampling rate can be designed based on the zero order hold equivalent of $P_{PZT}(s)$ at the sampling frequency $\frac{1}{T_f}$ and Eq.(9). Alternatively, if $C_{PZT}(s)$ is designed in the continuous domain, $C_{PZT}(z_1)$ may be obtained by applying an appropriate bilinear transformation. For implementation, the PES sampled at slow sampling frequency ($\frac{1}{T_s}$) must be repeated $N(=\frac{T_s}{T_f})$ times at the high sampling rate(Fig. 9) before feeding to the PZT actuator feedback controller $C_{PZT}(z_1)$. $C_{Pff}(z_1)$ is an approximate inverse of the zero order hold equivalent of $P_{PZT}(s)$ at the sampling frequency $\frac{1}{T_f}$.

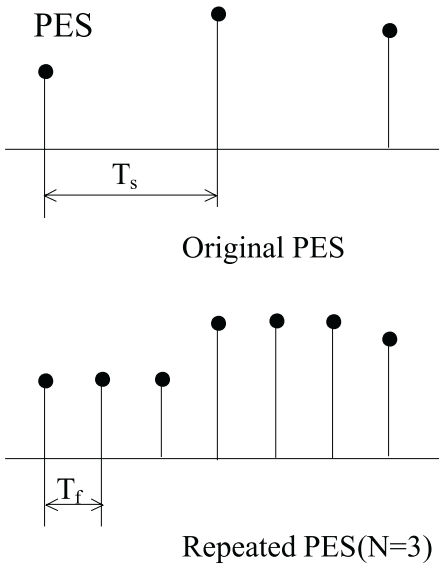

Figure 9: Position Error Signals(PESs) for Dual Rate Control

5 Initial Value Compensation for Dual Actuator System

In Mode Switching Control(MSC), the controller switches from track seeking control to track following control. In the beginning of the track following control phase, there may be a large overshoot and/or residual vibration due to the nonzero initial states of the VCM actuator at the switching instant. The large overshoot may even drive the PZT actuator out of its operating range ($\pm 1\mu$m). This section investigates how initial value compensation(IVC) may be applied to the dual actuator HDD system to improve the settling response when switching from track seeking control to track following control.

5.1 IVC for Parallel Track Following Control

The initial value compensation(IVC) design for the single actuator HDD system was proposed by Yamaguchi et al.[19]. Figure 10 shows the block diagram for parallel dual actutator track following control. In Fig.10, the VCM track following controller is represented by $C_{VCM}(z)$, and the PZT track following controller by $C_{PZT}(z)$. The VCM and PZT actuators are represented by $P_{VCM}(s)$ and $P_{PZT}(s)$, respectively. At the time of switching, the VCM

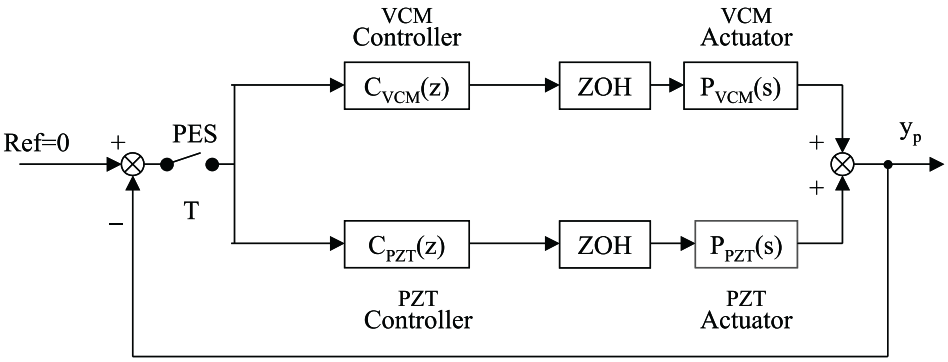

Figure 10: Block Diagram for Parallel Track Following Control

actuator has nonzero states. To develop the IVC scheme, the VCM and PZT actuators and controllers must be represented by discrete time states and output equations.

The VCM actuator is described by

$$\begin{aligned} x_v(k+1) &= A_v x_v(k) + B_v u_v(k),\ x_v(0) = x_{v0} \\ y_v(k) &= C_v x_v(k) \end{aligned} \tag{23}$$

where x_v is the VCM state, x_{v0} is the initial state, u_v denotes the input and y_v is the VCM actuator output. The dimension of x_v is assumed to be n_v and u_v and y_v are scalars.

The VCM controller is expressed as

$$\begin{aligned} x_{vc}(k+1) &= A_{vc} x_{vc}(k) + B_{vc}(r(k) - y(k)),\ x_{vc}(0) = x_{vc0} \\ u_v(k) &= C_{vc} x_{vc}(k) + D_{vc}(r(k) - y(k)) \end{aligned} \tag{24}$$

where x_{vc} is the VCM controller state, x_{vc0} is the initial state, $r - y$ is the sampled position error signal and is the input to the VCM controller. The dimension of x_{vc} is assumed to be n_{vc}.

The PZT actuator is described by

$$\begin{aligned} x_p(k+1) &= A_p x_p(k) + B_p u_p(k),\ x_p(0) = x_{p0} \\ y_p(k) &= C_p x_p(k) \end{aligned} \tag{25}$$

where x_p denotes the PZT state and x_{p0} is the initial state, u_p denotes the PZT plant input, and y_p is the position output of the PZT actuator. The dimension of x_p is denoted by n_p and u_p and y_p are scalars.

The PZT controller is expressed as

$$\begin{aligned} x_{pc}(k+1) &= A_{pc}x_{pc}(k) + B_{pc}(r(k) - y(k)),\ x_{pc}(0) = x_{pc0} \\ u_p(k) &= C_{pc}x_{pc}(k) + D_{pc}(r(k) - y(k)) \end{aligned} \tag{26}$$

where x_{pc} denotes the PZT controller state and x_{pc0} is the initial state. The dimension of x_{pc} is assumed to be n_{pc}.

The R/W head position is given by

$$y(k) = y_v(k) + y_p(k) \tag{27}$$

Assuming $r(k) = 0$ and that the tracking controllers for both VCM and PZT are turned on at $k = 0$, the total closed loop system is expressed as

$$\begin{aligned} x_{cl}(k+1) &= A_{cl}x_{cl}(k),\ x_{cl}(0) = x_{cl0} \\ y(k) &= C_{cl}x_{cl}(k) \end{aligned} \tag{28}$$

where:

$$A_{cl} = \begin{bmatrix} A_v - B_vD_{vc}C_v & B_vC_{vc} & -B_vD_{vc}C_p & 0 \\ -B_{vc}C_v & A_{vc} & -B_{vc}C_p & 0 \\ -B_pD_{pc}C_v & 0 & A_p - B_pD_{pc}C_p & B_pC_{pc} \\ -B_{pc}C_v & 0 & -B_{pc}C_p & A_{pc} \end{bmatrix} \tag{29}$$

$$C_{cl} = \begin{bmatrix} C_v & 0 & C_p & 0 \end{bmatrix} \tag{30}$$

$$x_{cl} = [x_v'\ x_{vc}'\ x_p'\ x_{pc}']' \tag{31}$$

From Eq.(28) and (29), the transform domain expression for $y(k)$ is obtained from

$$y(z) = C_{cl}X_{cl}(z) = C_{cl}z(zI - A_{cl})^{-1}x_{cl0} \tag{32}$$

We define $B_{cli}(i = 1, ..., 4)$ by

$$B_{cl} = [B_{cl1} \vdots B_{cl2} \vdots B_{cl3} \vdots B_{cl4}] = \begin{bmatrix} I_{n_v} & 0 & 0 & 0 \\ 0 & I_{n_{vc}} & 0 & 0 \\ 0 & 0 & I_{n_p} & 0 \\ 0 & 0 & 0 & I_{n_{pc}} \end{bmatrix} \tag{33}$$

Then noticing $(zI - A_{cl})^{-1} = adj(zI - A_{cl})/|zI - A_{cl}|$, Eq. (32) can be expressed as

$$\begin{aligned} y(z) &= \frac{zC_{cl}adj(zI - A_{cl})B_{cl1}}{|zI - A_{cl}|}x_{v0} + \frac{zC_{cl}adj(zI - A_{cl})B_{cl2}}{|zI - A_{cl}|}x_{vc0} \\ &+ \frac{zC_{cl}adj(zI - A_{cl})B_{cl3}}{|zI - A_{cl}|}x_{p0} + \frac{zC_{cl}adj(zI - A_{cl})B_{cl4}}{|zI - A_{cl}|}x_{pc0} \end{aligned} \tag{34}$$

In IVC, the initial states of the VCM and PZT controllers, x_{vc0} and x_{pc0}, are adjusted as functions of the measured or estimated initial states of VCM and PZT, x_{v0} and x_{p0}, to make the response as desired. In the disk drive servo, the position error signal is the only signal available for the determination of x_{v0} and x_{p0}. Furthermore, PZT is saturated most of time during seek, its operating range is limited and it can respond fast. Thus, it is best to ignore the initial state of x_{p0} or to assume $x_{p0} = 0$, and use PES for determination of x_{v0}.

The objective of IVC is then to specify the initial states of the VCM and PZT controllers to minimize the effect of the nonzero initial states of the VCM actuator on the position error signal at the completion of settling phase.

5.1.1 IVC Design by Pole-Zero Cancellation

For $x_{p0} = 0$, Eq.(35) may be rewritten as

$$y_z = \frac{zN_v(z)}{D(z)}x_v(0) + \frac{zN_{vc}(z)}{D(z)}x_{vc}(0) + \frac{zN_{pc}(z)}{D(z)}x_{pc}(0) \tag{35}$$

where

$$\begin{aligned} D(z) &= |zI - A_{cl}| \\ N_v(z) &= C_{cl}adj(zI - A_{cl})B_{cl1} \\ N_{vc}(z) &= C_{cl}adj(zI - A_{cl})B_{cl3} \\ N_{pc}(z) &= C_{cl}adj(zI - A_{cl})B_{cl4} \end{aligned} \tag{36}$$

In Eq.(35), $D(z)$ is a scalar z polynomial equation and $N_v(z)$, $N_{vc}(z)$ and $N_{pc}(z)$ are $1\times n_v$,$1\times n_{vc}$ and $1\times n_{pc}$ polynomial matrices respectively. By introducing $n_{vc}\times n_v$ and $n_{pc}\times n_v$ real coefficient matrix K_v and K_p, the initial states of the VCM and PZT contollers are assigned as

$$\begin{aligned} x_{vc}(0) &= K_v x_v(0) \\ x_{pc}(0) &= K_p x_v(0) \end{aligned} \tag{37}$$

Substituting Eq. (37) into Eq. (35),

$$\begin{aligned} y(z) &= \frac{zN_v(z)}{D(z)}x_v(0) + \frac{zN_{vc}(z)}{D(z)}K_v x_v(0) + \frac{zN_{pc}(z)}{D(z)}K_p x_v(0) \\ &= z\frac{N_v(z)+N_{vc}(z)K_v+N_{pc}(z)K_p}{D(z)}x_v(0) \end{aligned} \tag{38}$$

Let λ_j's denote the characteristic roots of $D(z)$. Assuming that any λ_j does not repeat, $y(z)$ can be written as

$$y(z) = \sum_{j=1}^{N}\frac{R_j}{(z-\lambda_j)} \tag{39}$$

where $N = n_v + n_{vc} + n_p + n_{pc}$ and

$$R_j = (z-\lambda_j)z\frac{N_v(z)+N_{vc}(z)K_v+N_{pc}(z)K_p}{D(z)}\bigg|_{z=\lambda_j} x_{v0} \tag{40}$$

Note that if K_v and K_p are selected so that $N_v(\lambda_j)+N_{vc}(\lambda_j)K_v+N_{pc}(\lambda_j)K_p = 0$, The response $y(k)$ does not contain a mode associated with the characteristic root λ_j.

Rewrite N_v,N_{vc},N_p and $x_v(0)$ as following:

$$\begin{aligned} N_v &= [N_{v_1}, N_{v_2}, ..., N_{v_{n_v}}] \\ N_{vc} &= [N_{vc_1}, N_{vc_2}, ..., N_{v_{n_{vc}}}] \\ N_{pc} &= [N_{vp_1}, N_{vp_2}, ..., N_{v_{n_{pc}}}] \\ x_v(0) &= [x_{v_1}(0), x_{v_2}(0), ..., x_{v_{n_v}}(0)]' \end{aligned} \tag{41}$$

Then Eq. (38) can be expanded as:

$$
\begin{aligned}
y(z) = \quad & z \cdot D(z)^{-1} \\
& \times \{[k_{v_{11}} N_{vc_1} + k_{v_{21}} N_{vc_2} + ... + k_{v_{n_{vc}1}} N_{n_{vc}} + ... \\
& k_{p_{11}} N_{pc_1} + k_{p_{21}} N_{pc_2} + ... + k_{p_{n_{pc}1}} N_{n_{pc}} + N_{v_1}] x_{v_1}(0) + ... \\
& + [k_{v_{1n_v}} N_{vc_1} + k_{v_{2n_v}} N_{vc_2} + ... + k_{v_{n_{vc}n_v}} N_{n_{vc}} + .. + \\
& k_{p_{1n_v}} N_{pc_1} + k_{p_{2n_v}} N_{pc_2} + ... + k_{p_{n_{pc}n_v}} N_{n_{pc}} + N_{v_{n_v}}] x_{v_{n_v}}(0)\}
\end{aligned} \tag{42}
$$

where $k_{v_{ij}}$ and $k_{p_{ij}}$ is the (i,j) entry of the matrices K_v and K_p, respectively. Assume that the undesird characteristic roots in $D(z)$ are $\lambda_k (k = 1, .., r)$. i.e. they make the transient response poor after the dual actuator servo system is switched from track seeking control to track following control. From Eq.(42), the following matrix equation should be satisfied for each $j (j = 1, ..., n_v)$ in order to make the response $y(k)$ free from all the undesired modes.

$$
\begin{bmatrix}
N_{vc_1}(\lambda_1) & \cdots & N_{vc_{n_{vc}}}(\lambda_1) & N_{pc_1}(\lambda_1) & \cdots & N_{pc_{n_{pc}}}(\lambda_1) \\
N_{vc_1}(\lambda_2) & \cdots & N_{vc_{n_{vc}}}(\lambda_2) & N_{pc_1}(\lambda_2) & \cdots & N_{pc_{n_{pc}}}(\lambda_2) \\
 & & & \cdot & & \\
 & & & \cdot & & \\
 & & & \cdot & & \\
N_{vc_1}(\lambda_r) & \cdots & N_{vc_{n_{vc}}}(\lambda_r) & N_{pc_1}(\lambda_r) & \cdots & N_{pc_{n_{pc}}}(\lambda_r)
\end{bmatrix}
\begin{bmatrix}
k_{v_{1j}} \\ k_{v_{2j}} \\ \cdot \\ \cdot \\ \cdot \\ k_{p_{n_{pc}j}}
\end{bmatrix}
= \begin{bmatrix}
-N_{v_j}(\lambda_1) \\ -N_{v_j}(\lambda_2) \\ \cdot \\ \cdot \\ \cdot \\ -N_{v_j}(\lambda_r)
\end{bmatrix}
\tag{43}
$$

Notice that corresponding to each entry of the VCM initial state $x_{v_j}(0) (j = 1, ..., n_v)$, there are associated unknowns $k_{v_{ij}}$ $(i = 1, ..., n_{vc})$ and $k_{p_{ij}}$ $(i = 1, ..., n_{pc})$. If $n_{vc} + n_{pc} \geq r$ and any λ_j doesn't repeat, a solution exists for the above matrix equation[19], i.e. K_v and K_p can be found for IVC of the dual actuator system.

5.2 IVC for Decoupled Track Following Control

In decoupled tracking following control, the VCM path does not see the PZT path. Only the VCM controller is assigned initial values to cancel the undesired modes due to the nonzero initial states of the VCM actuator. The PZT actuator is used to suppress the disturbance for achieving superior performance. Notice that the IVC design for this decoupled track following control scheme is similar to the single actuator IVC design[19]. In order to achieve a smooth transient response, the PZT actuator should be "softly" switched on.

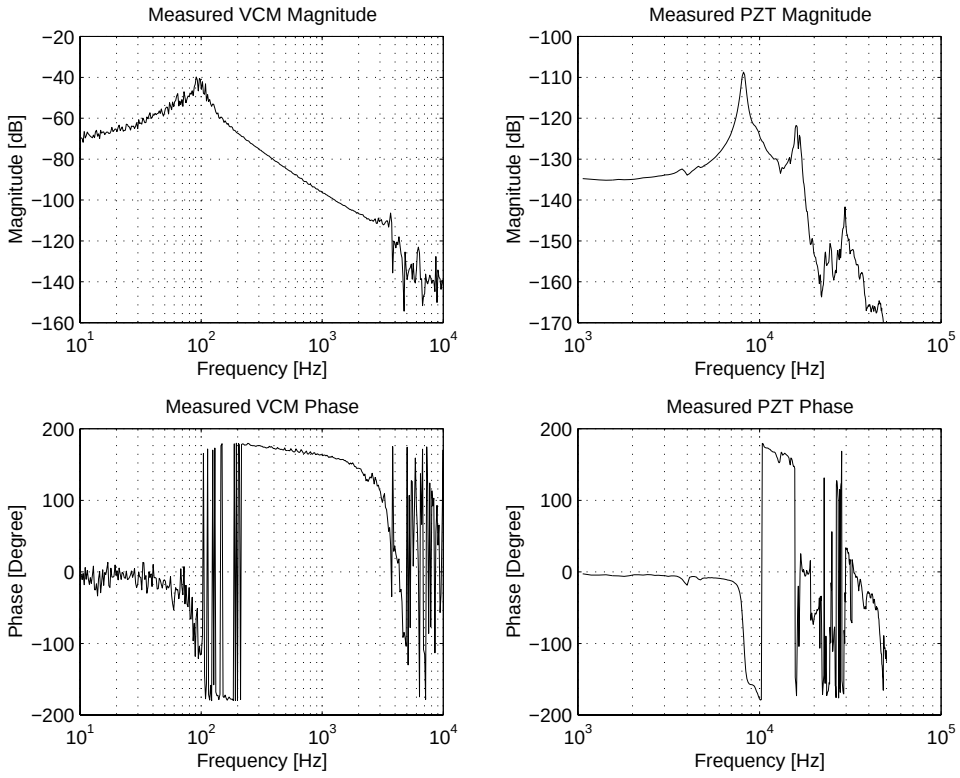

Figure 11: Measured VCM and PZT Frequency Responses

6 Design Example

6.1 RTRD Settling Design

In this section, we present a design example of the dual actuator setting controllers. The design specification is to achieve an $1.0kHz$ or higher bandwidth, an about 40° phase margin and a $4dB$ or larger gain margin. The spindle speed is 7208rpm. The sampling frequency for the VCM controller is $10.9kHz$ corresponding to 84 sectors each track, and the fast sampling frequency for the PZT controller is $30.3kHz$ corresponding to 262 sectors each track. In single rate dual actuator settling, the two controllers work at the slow sampling frequency. In dual rate dual actuator settling, the VCM controller works at the slow sampling frequency and the PZT controller at the high sampling frequency.

Figure 11 shows measured VCM and PZT actuator frequency characteristics of the Hitachi prototype dual actuator HDD system[18]. Figure 12 shows the measured PZT actuator

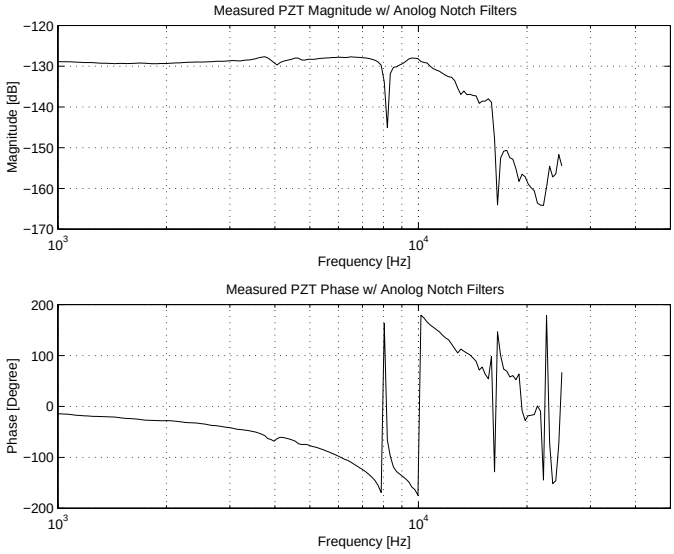

Figure 12: Measured PZT Frequency Response with Notch Filters

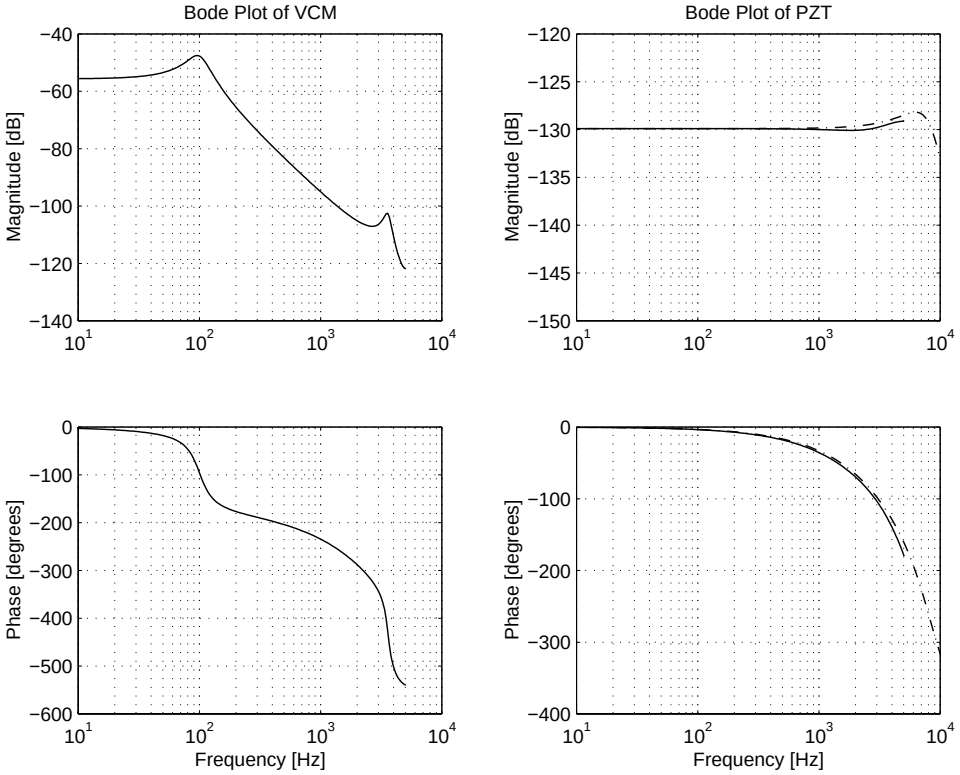

Figure 13: Bode plots of Dual Actuators

frequency characteristics with notch filters at $8.2kHz$ and $16kHz$. Figure 13 is the Bode plots of the VCM and PZT actuator models. For the PZT actuator in Fig.13, the solid line corresponds to the frequency response under slow ampling frequency and the dash line the frequency response under fast ampling frequency. The VCM magnitude has a resonant peak at $3.1kHz$. The phase of VCM is close to -180° around $600Hz$ due to the effect of double integrator. The PZT frequency response is flat with phase lag close to zero at low frequencies and increasing at high frequencies due to the resonant frequency at $8.2kHz$. Notice that in Fig.13, the frequency responses of the VCM an PZT actuators both include notch filters implemented by analog circuits.

The VCM feedback controller used in single rate and dual rate control is:

$$C_{VCM}(z) = 1.4446\frac{(z-0.8664)(z-0.1447)}{z^2+0.1659z+0.1813} \tag{44}$$

The VCM feedforward controller is a constant gain, which is the mass of the VCM actuator:

$$C_{Vff}(z) = 1.5365e-3 \tag{45}$$

The PZT feedback controller is given by:

$$C_{PZT}(z) = 4.300\frac{(z-1)(z-0.1247)}{(z-0.9939)(z-0.9396)} \tag{46}$$

This PZT controller has a zero at 1 so that the frequency response gain of PZT path is low at low frequencies but is relatively high from $100Hz$ to $1kHz$.

Since the frequency response of the PZT actuator is flat at low frequencies , the PZT estimator is approximated by a constant with one step delay(Eq.47) and the PZT feedforward controller is a constant, which is the inverse of the DC gain of the PZT actuator (Eq.48).

$$E_{PZT}(z) = 2.4 \times 10^{-7} z^{-1} \tag{47}$$

$$C_{Pff}(z) = \frac{1}{2.4} \times 10^7 \tag{48}$$

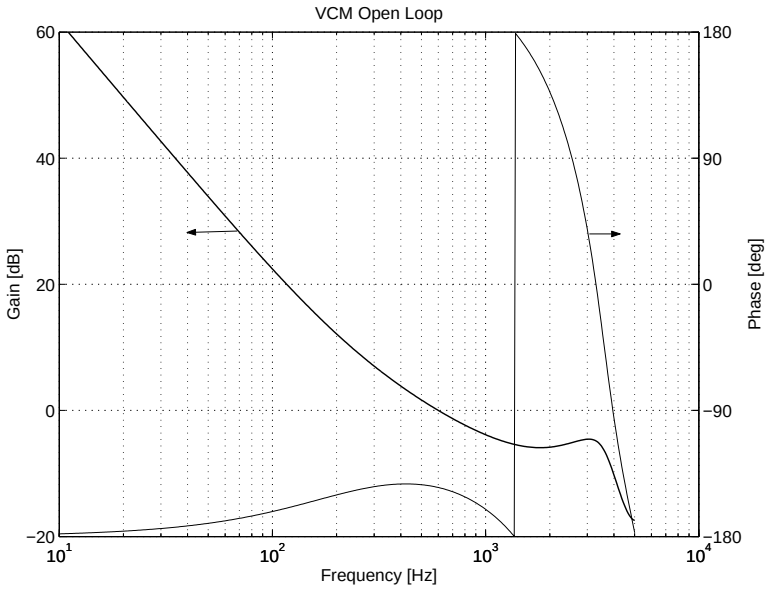

Figure 14: VCM Open Loop Frequency Response

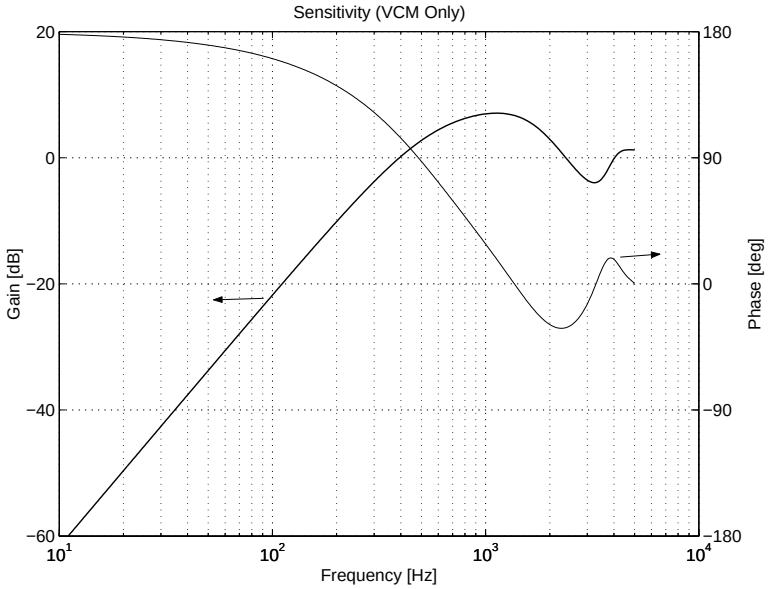

Figure 15: VCM Sensitivity Function

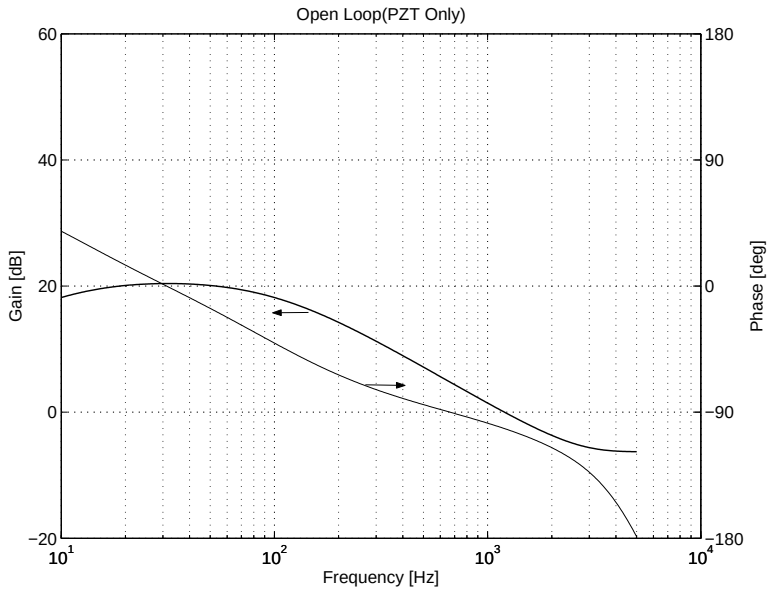

Figure 16: PZT Open Loop Frequency Response

When the PZT controller is deactivated, the VCM settling controller provides(Fig.14) a crossover frequency at $600Hz$, a gain margin of $5.39dB$ and a phase margin of $35°$ (notice that VCM loop is stable). Figure 15 shows the sensitivity function of the VCM loop.

Figure 16 and 17 show the PZT open loop frequency response and sensitivity function, respectively. The PZT open loop transfer function has a crossover frequency at $1200Hz$, a gain margin of $6.28dB$ and a phase margin of $78.3°$

The ratio(R) of the VCM equivalent path and the PZT path is given in Fig. 18. From this figure, the magnitude of R is large at low frequencies and small at high frequencies. When the magnitude of R is close to one, the phase is about $73.2°$, which is far from $\pm 180°$.

Figure 19 is the total open loop frequency response; the dual actuator design achieves a crossover frequency at $1.1kHz$, a phase margin of $33.9°$ and a gain margin about of $5.1dB$.

Figure 20 shows three sensitivity functions: the solid line corresponds to the dual actuator sensitivity, the dot line to the PZT loop sensitivity and the dash line to the single VCM loop sensitivity. The dual actuation achieves better disturbance rejection compared to VCM actuator only. Figure 21 shows the complementary sensitivity functions.

When the PZT controller is "softly" switched on by the time varying parameter $\alpha(t)$, the

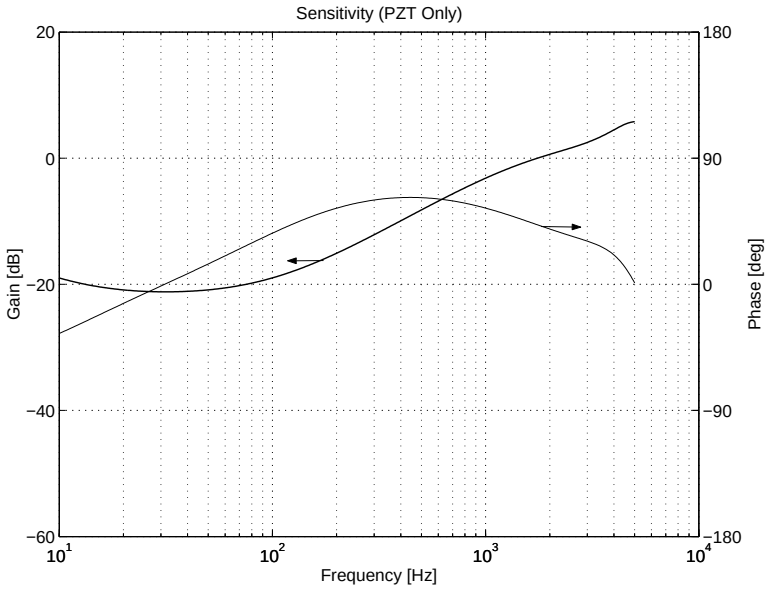

Figure 17: PZT Sensitivity Function

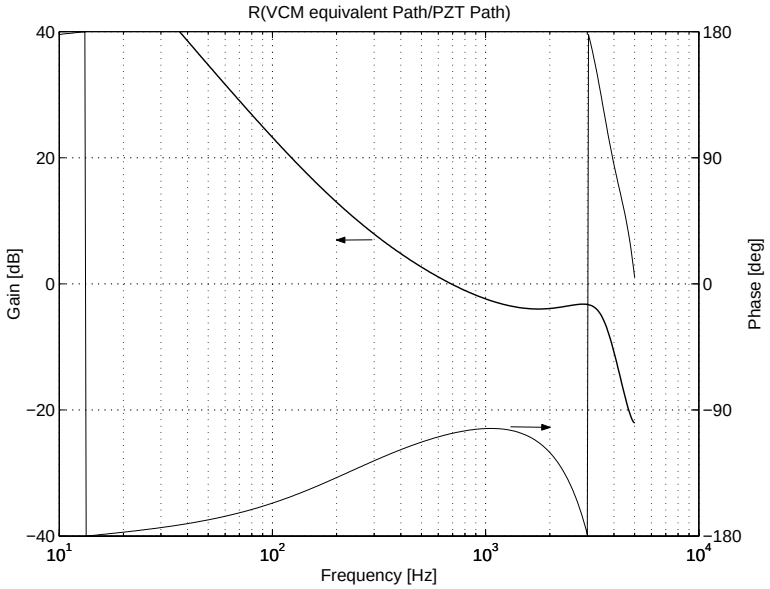

Figure 18: Relative Magnitude between VCM Equivalent Path and PZT Path

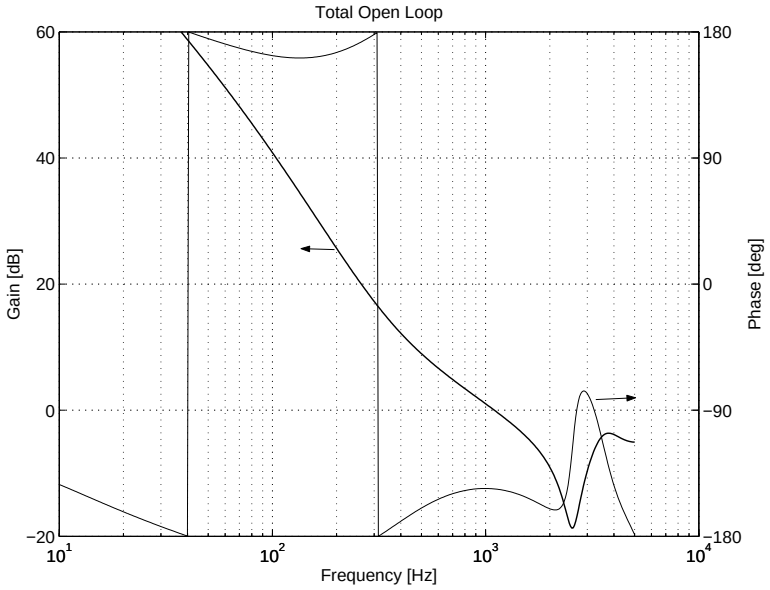

Figure 19: Total Open Loop Frequency Response

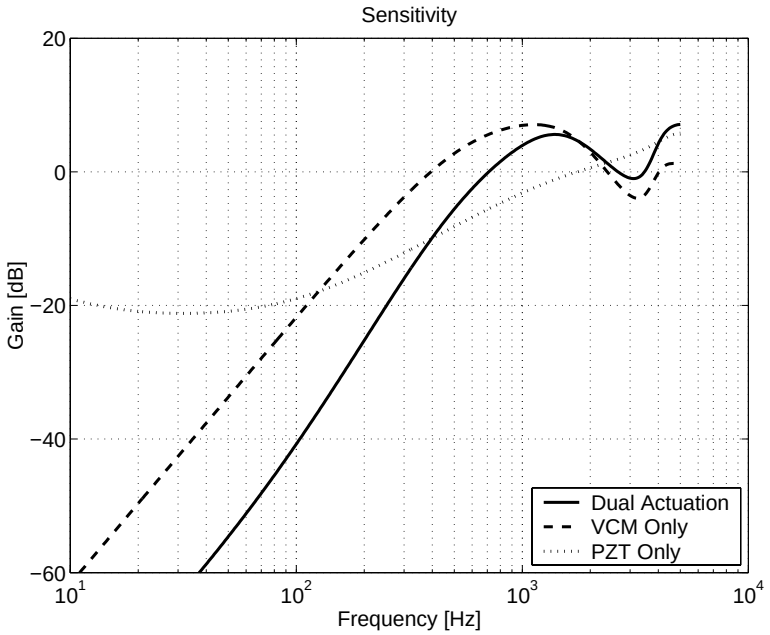

Figure 20: Sensitivity Functions

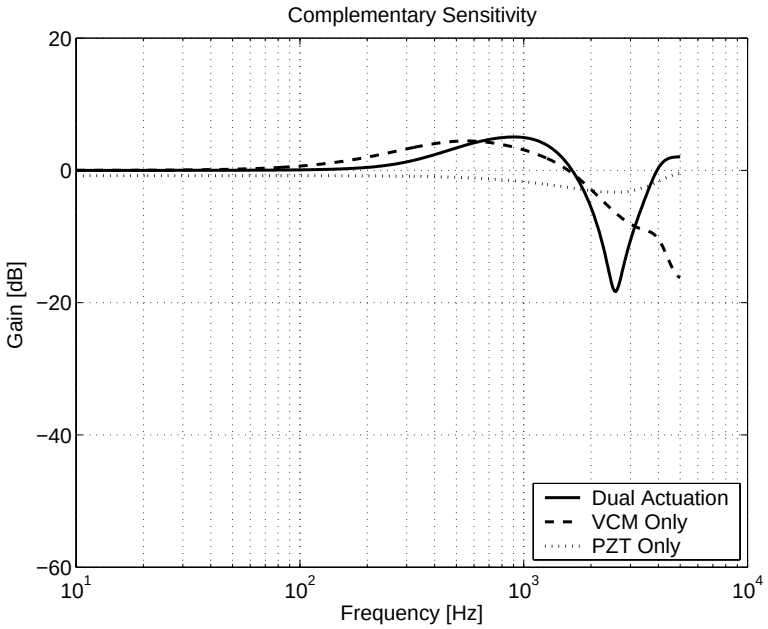

Figure 21: Complementary Sensitivity Functions

open loop frequency response of the dual actuator system in Fig.22. Table 3 shows the gain and phase margins corresponding to different α's.

Table 3: Gain and Phase Margins($\alpha \in$[0 1])

α	0	0.25	0.5	0.75	1
Gain Margin	$5.39dB$	$5.81dB$	$6.96dB$	$9.36dB$	$5.1dB$
Phase Margin	35°	30.6°	30.4°	31.6°	33.85°

In dual rate RTRD settling control, the PZT feedforward controller $C_{Pff}(z_1)$ is also a constant, the same as the single rate RTRD settling design. The PZT feedback controller $C_{PZT}(z_1)$ working at high sampling frequency($\frac{1}{T_f}$) is

$$C_{PZT}(z_1) = 4.300\frac{(z_1-1)(z_1-0.7016)}{(z_1-0.9979)(z_1-0.9795)} \tag{49}$$

6.2 Initial Value Compensation for Parallel Track Following Control

The parallel track following controller has been designed in [21]. The VCM and PZT tracking following controllers(sampling frequency $\frac{1}{T_s}$) are:

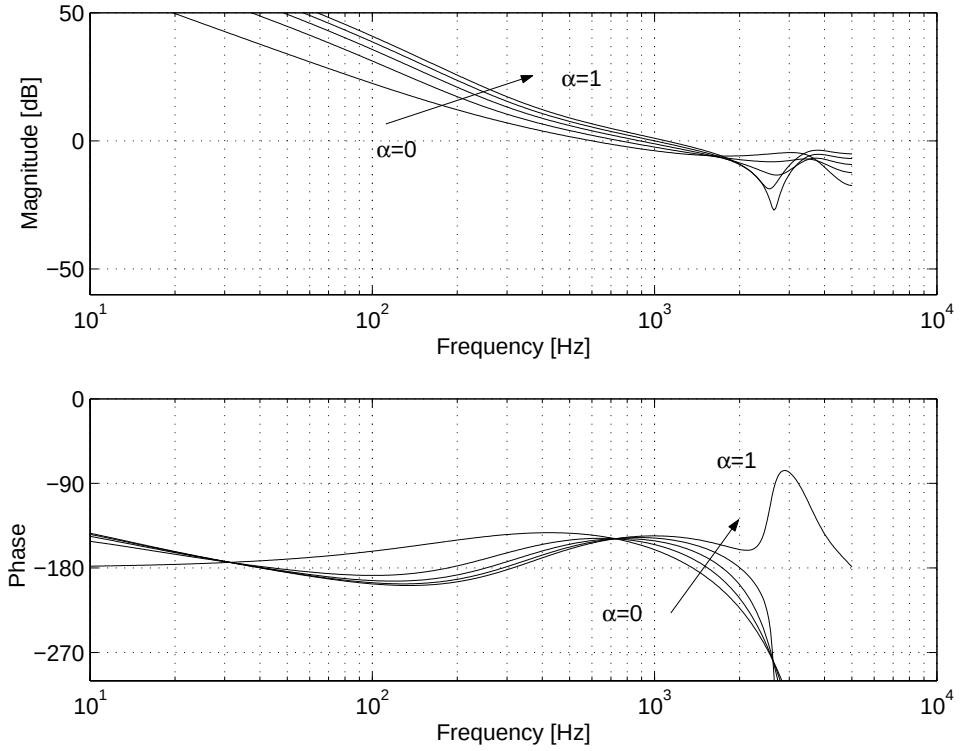

Figure 22: Open Loop Frequency Responses of Dual Actuator System under Soft Switching

$$C_{VCM}(z) = 0.1691\frac{(z-0.8556)^2(z-0.6214)}{(z-1)(z-0.5623)(z+0.3709)} \tag{50}$$

$$C_{PZT}(z) = 2.8179\frac{(z-1)(z-0.1247)}{(z-0.9396)(z-0.9938)} \tag{51}$$

The closed loop pole-zero map is shown in Fig.23. The track following closed loop poles are: $-0.4410+0.1915i$,$-0.4410-0.1915i$, $0.1128+0.5906i$ $0.1128-0.5906i$,$0.0210+0.3978i$, $0.0210-0.3978i$ $0.0643+0.0742i$, $0.0643-0.0742i$, 0.5953 $0.9513+0.1084i$, $0.9513-0.1084i$, 0.9657 and 0.9935.

As shown in Fig.23, there are four poles close to the unit circle, which makes the transient response poor. The IVC design is to find K_v and K_p so that these four poles(characteristic

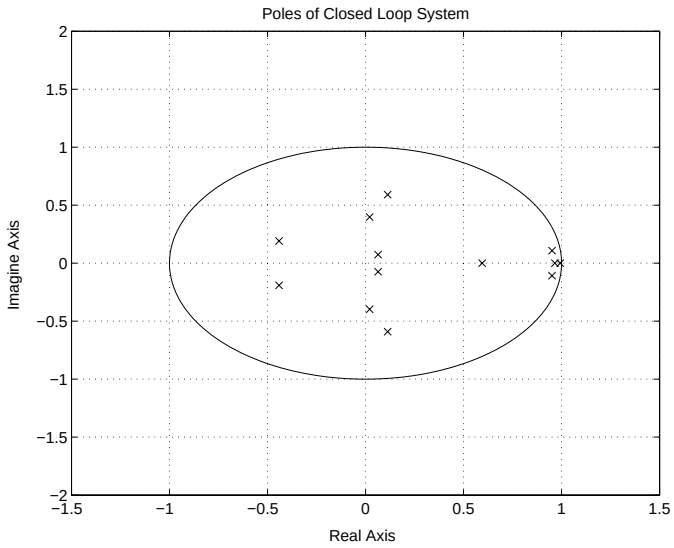

Figure 23: Pole-zero map of Parallel Closed Loop System

roots) do not affect the transient response. The four characteristic roots are

$$\begin{aligned}\lambda_1 &= 0.9513 + 0.1084i \\ \lambda_2 &= 0.9513 - 0.1084i \\ \lambda_3 &= 0.9557 \\ \lambda_4 &= 0.9935 \end{aligned} \tag{52}$$

Substitute λ_i's$(i = 1, ..., 4)$ into the matrix equation(Eq.43) for the VCM actuator states x_{v_1} and x_{v_2}, corresponding to the VCM actuator position and velocity. Soving the resulting equations for $K_{v3\times 2}$ and $K_{p1\times 1}$, we obtain

$$\begin{aligned} k_{v_{11}} &= -5.5768e4 \\ k_{v_{21}} &= 1.1479e5 \\ k_{v_{31}} &= -5.885e4 \\ k_{p_{11}} &= -2.8708e3 \end{aligned} \tag{53}$$

$$
\begin{aligned}
k_{v_{12}} &= -2.9319e1 \\
k_{v_{22}} &= 4.9920e1 \\
k_{v_{32}} &= -2.0583e1 \\
k_{p_{12}} &= -2.9701e-1
\end{aligned} \tag{54}
$$

6.3 Initial Value Compensation for Decoupled Track Following Control

In decoupled track following control, the VCM controller is

$$
C_{VCM}(z) = 0.1824\frac{(z-0.8995)^2(z-0.6214)}{(z-1)(z-0.4594)(z+0.3709)} \tag{55}
$$

The poles of the VCM loop are:

$$
\begin{aligned}
\lambda_1 &= 9.3612e-01 \\
\lambda_2 &= 8.5529e-01+1.7648e-01i \\
\lambda_3 &= 8.5529e-01-1.7648e-01i \\
\lambda_4 &= 4.5352e-01+4.1746e-01i \\
\lambda_5 &= 4.5352e-01-4.1746e-01i \\
\lambda_6 &= -4.6075e-01+2.1692e-01i \\
\lambda_7 &= -4.6075e-01-2.1692e-01i \\
\lambda_8 &= -1.8793e-01
\end{aligned}
$$

Notice that the first three poles are close to the unit circle, and the corresponding response modes should be eliminated in the IVC design.

Substitute λ_i's$(i = 1, ..., 3)$ into the matrix equation(Eq.43) for the VCM actuator states x_{v_1} and x_{v_2}, corresponding to the VCM actuator position and velocity. Soving the equations for $K_{v3\times 2}$, we obtain

$$
\begin{aligned}
k_{v_{11}} &= -1.3531e4 \\
k_{v_{21}} &= 4.2865e4 \\
k_{v_{31}} &= -2.8497e4
\end{aligned} \tag{56}
$$

and

$$
\begin{aligned}
k_{v_{12}} &= -2.5584e1 \\
k_{v_{22}} &= 4.1634e1 \\
k_{v_{32}} &= -1.5959e1
\end{aligned} \tag{57}
$$

Notice that initial values are assigned to the VCM actuator controller only.

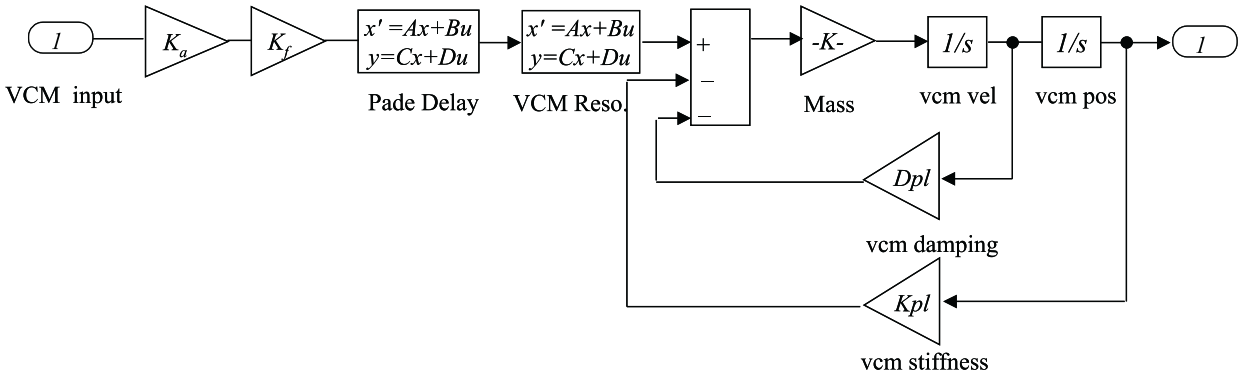

Figure 24: VCM Simulink Model

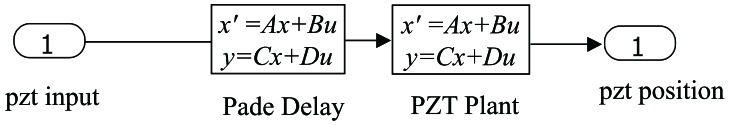

Figure 25: PZT Simulink Model

7 Simulation Result

The simulated disk drive has specifications in Table 4.

Table 4: Parameters of Simulated Disk Drive

Capcity	$18.4GB$
Disks	$5/3.5"$
TPI	$13,000$
Spindle Speed	$7,208rpm$
Sampling Period	$99.1\mu s(slow)/33.0\mu s(fast)$
Average Seek Time	$6.5/7.5ms$(Read/Write)

Figure 24 and 25 show the matlab simulink VCM and PZT models, respectively. The VCM simulation model includes the power amplifier gain (K_a) , the current to force conversion gain (K_f) , a second order system with a Pade delay approximation and a resonance mode. The PZT simulation model is a second order system with a Pade delay approximation.

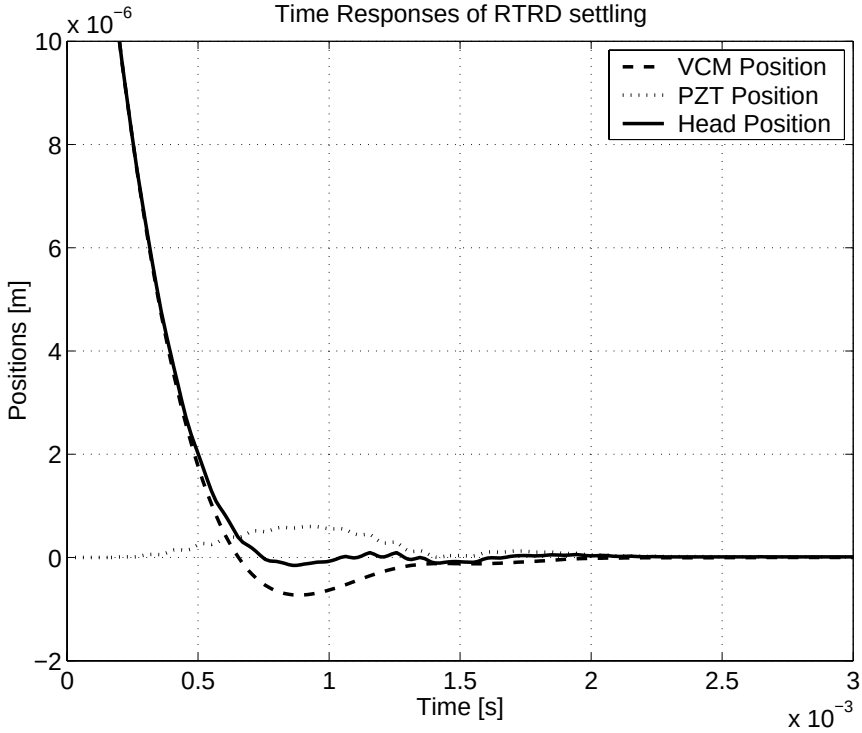

Figure 26: Dual Actuator Reference Settling Simulation

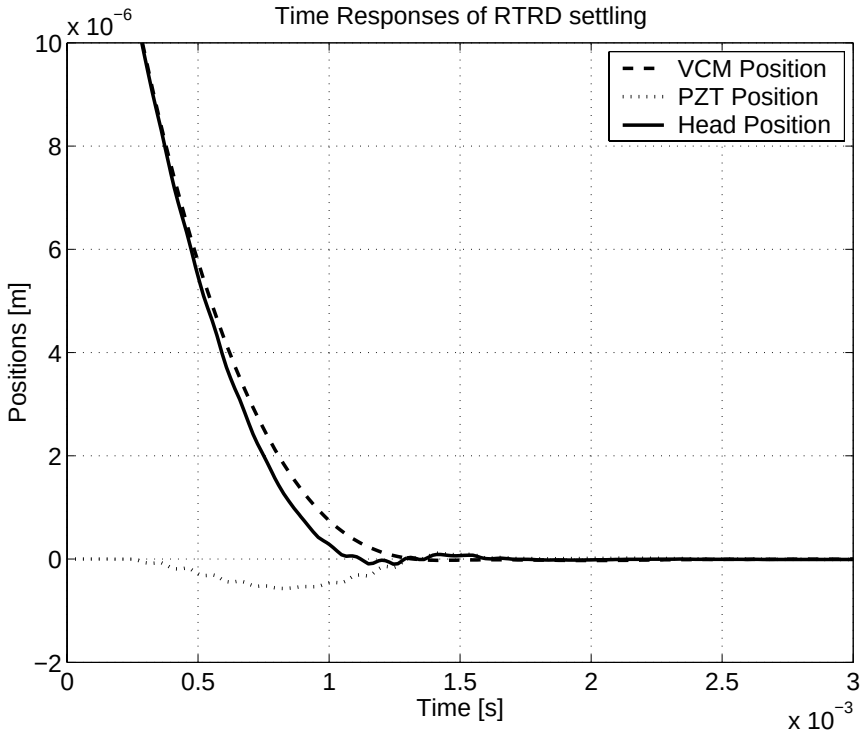

Figure 27: Dual Actuator Reference Settling Simulation

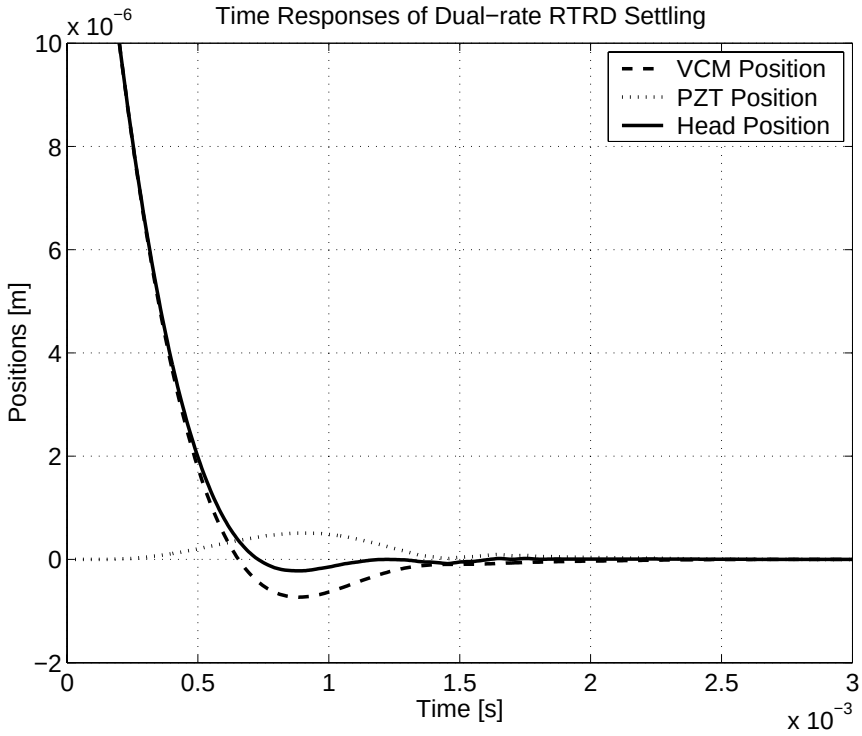

Figure 28: Dual Actuator Reference Settling Simulation

7.1 RTRD Settling Simulation

Figure 26 shows a settling simulation with the VCM initial values $[a_{VCM}(0), v_{VCM}(0), p_{VCM}(0)]$ $= [100m/s^2, -60mm/s, 20\mu m]$. The solid line corresponds to the R/W head position, the dash line corresponds to the VCM actuator position and the dotted line corresponds to the PZT actuator position. In this dual reference scheme, it takes about $0.7ms$ for the R/W head to settle down on the target track compared to about $1.5ms$ with only VCM settling reference. Figure 27 shows a settling simulation with the VCM initial values $[a_{VCM}(0), v_{VCM}(0), p_{VCM}(0)] =$ $[70m/s^2, -40mm/s, 19\mu m]$. The solid line corresponds to the R/W head position, the dash line corresponds to the VCM actuator position and the dotted line corresponds to the PZT actuator position. The settling time is further shortened by about $0.25ms$ compared to the scheme with only VCM reference.

Figure 28 shows a reference settling simulation with the PZT actuator updated 3 times faster than the VCM actuator. The VCM actuator initial values are $[a_{VCM}(0), v_{VCM}(0), p_{VCM}(0)]$

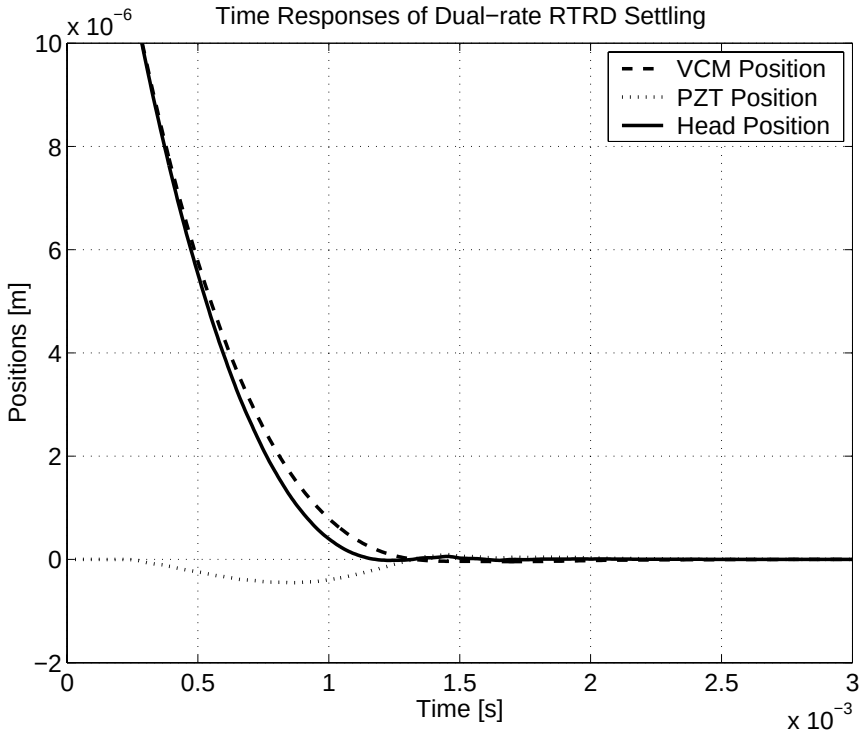

Figure 29: Dual Actuator Reference Settling Simulation

$= [100m/s^2, -60mm/s, 20\mu m]$. The solid line corresponds to the R/W head position, the dash line corresponds to the VCM actuator position and the dotted line corresponds to the PZT actuator position. The dual rate scheme achieves smoother transient response compared to the single rate scheme. Figure 29 shows a reference settling simulation with the PZT actuator updated 3 times faster than the VCM actuator with the VCM actuator initial values $[a_{VCM}(0), v_{VCM}(0), p_{VCM}(0)] = [70m/s^2, -40mm/s, 19\mu m]$.

7.2 IVC Settling Simulation for Parallel Track Following

In this section, simulation results are shown for the settling phase of a typical MSC system. It is assumed that the settling phase starts at $t = 0$.

Figure 30 shows simulated response without IVC. The VCM intial values are $[v_{VCM}(0), p_{VCM}(0)] = [-6mm/s, 1\mu m]$ and the PZT actuator is assumed to have enough moving range. The solid line corresponds to the R/W head position, the dash line corresponds to the VCM actuator position and the dotted line corresponds to the PZT actuator position. Both VCM

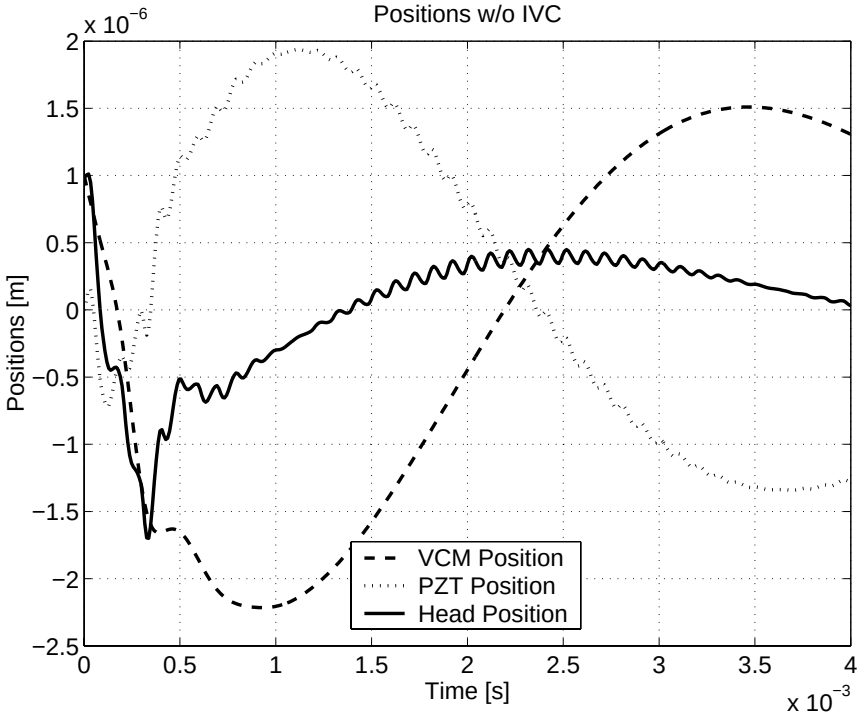

Figure 30: Dual Actuator IVC Settling Simulation

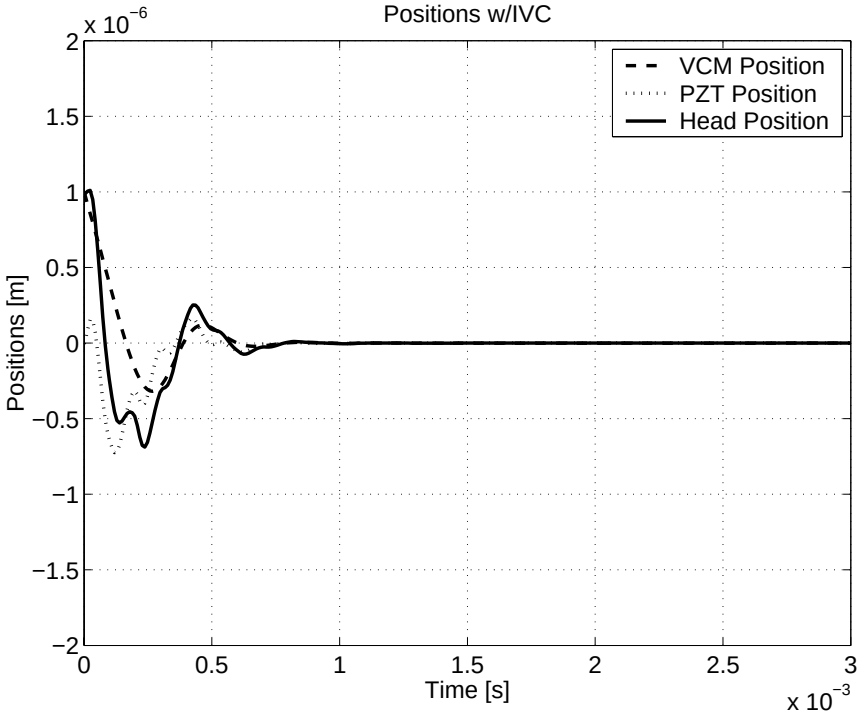

Figure 31: Dual Actuator IVC Settling Simulation

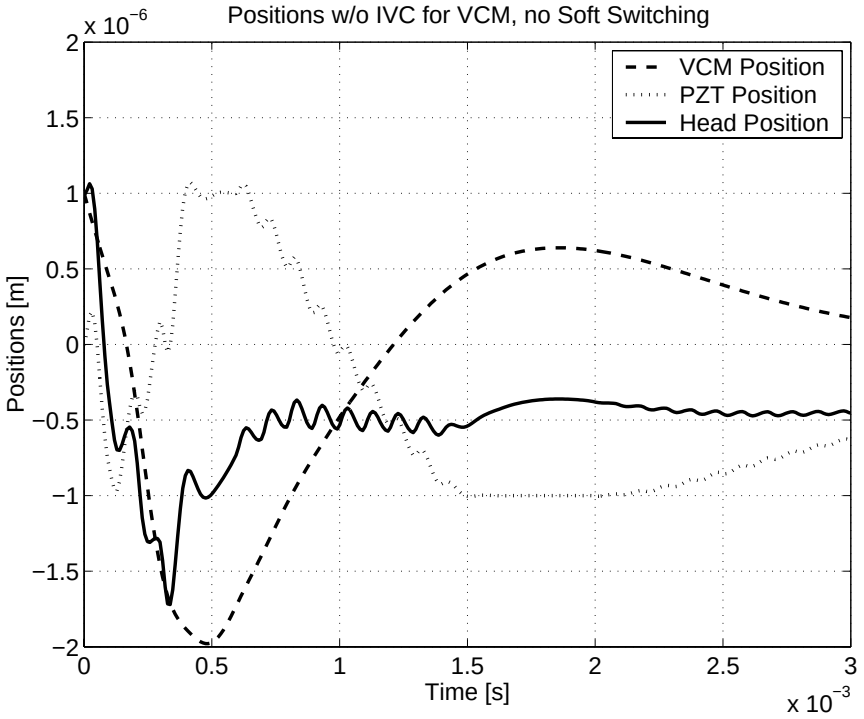

Figure 32: Dual Actuator Settling Simulation

and PZT actuator have a long transient period and residual oscilations without IVC. The R/W head takes quite a long time to settle down($> 3ms$).

Figure 31 shows simulated responses with IVC. The VCM intial values are $[v_{VCM}(0), p_{VCM}(0)] = [-6mm/s, 1\mu m]$. The solid line corresponds to the R/W head position, the dash line corresponds to the VCM actuator position and the dotted line corresponds to the PZT actuator position. Both VCM and PZT actuator have much less residual oscilations with IVC. The PZT response is within the operating range($1\mu m$).The head settles down in about $0.4ms$.

7.3 IVC Settling Simulation for Decoupled Track Following

Figure 32 shows simulated responses without IVC and soft switching. The VCM intial values are $[v_{VCM}(0), p_{VCM}(0)] = [-6mm/s, 1\mu m]$. The solid line corresponds to the R/W head position, the dash line corresponds to the VCM actuator position and the dotted line corresponds to the PZT actuator position. Both the VCM and PZT actuator have large residual vibration due to the VCM actuator initial values.

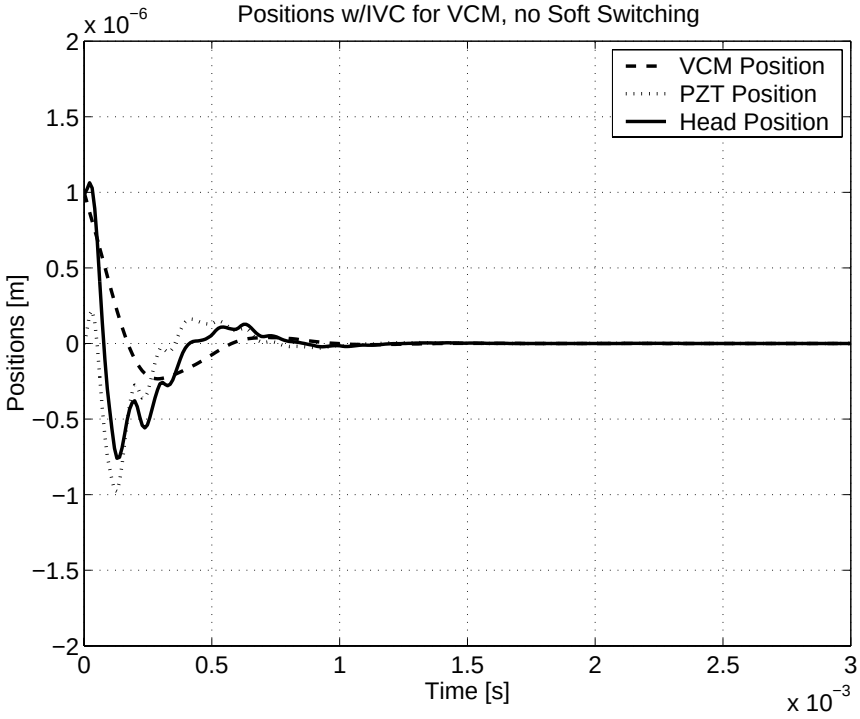

Figure 33: Dual Actuator Settling Simulation

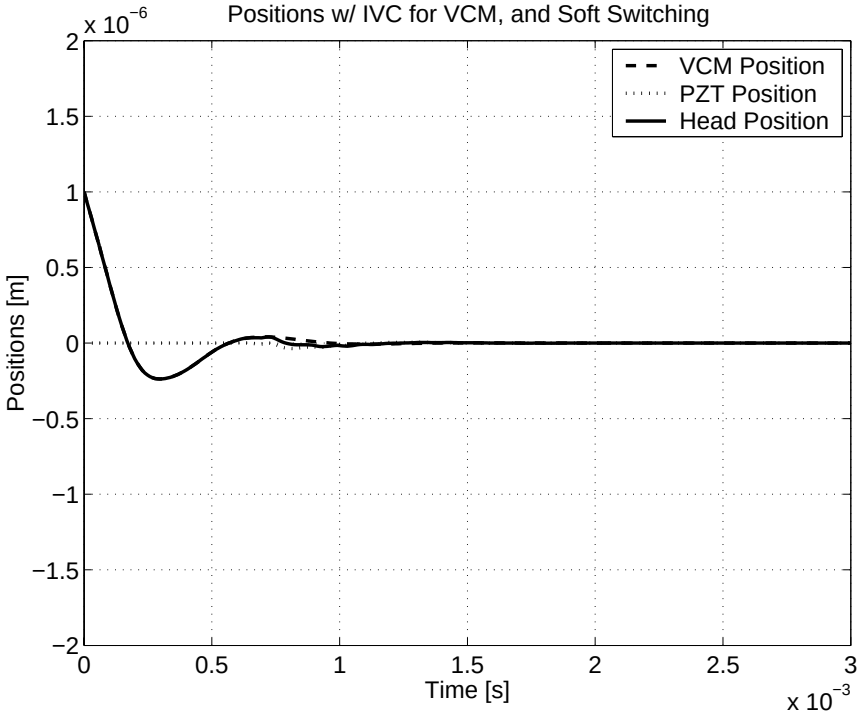

Figure 34: Dual Actuator Settling Simulation

Figure 33 shows simulated responses with IVC but no soft switching. The VCM intial values are $[v_{VCM}(0),p_{VCM}(0)] = [-6mm/s,1\mu m]$. The solid line corresponds to the R/W head position, the dash line corresponds to the VCM actuator position and the dotted line corresponds to the PZT actuator position. Both the VCM and PZT actuators have significantly reduced residual oscilations. The head settles down in about $1ms$. The PZT actuator has quite a large overshoot in the beginning of settling.

Figure 34 shows simulated responses with IVC and soft switching. The VCM intial values are $[v_{VCM}(0),p_{VCM}(0)] = [-6mm/s,1\mu m]$. The solid line corresponds to the R/W head position, the dash line corresponds to the VCM actuator position and the dotted line corresponds to the PZT actuator position. Both the VCM and PZT actuators have reduced residual oscilations. The head settles down in about $0.7ms$. Because of soft switching of the PZT loop, the PZT actuator has very small motion in the beginning of settling.

8 Conclusion

In this report, two settling schemes for dual actuation of R/W head positioning are discussed: the reference trajectory re-design(RTRD) scheme and the IVC scheme. The settling performace is improved when two reference signals are introduced to give the reference signal for each of VCM and PZT actuators. Soft switching is used for the PZT actuator to avoid exciting unmodeled high frequency dynamics. In the dual rate RTRD scheme, the reference signal for PZT actuator is updated at a high frequency resulting in smoother transient responses. IVC improves the settling transient response for both the parallel and decoupled track following structures. The performance of IVC for the decoupled track following structure is further improved by introduing soft switching for the PZT actuator.

Acknowledgements

This research was conducted at the Computer Mechanics Laboratory(CML) in the Department of Mechanical Engineering, University of California at Berkeley. The authors would like to thank Mr. H.Numasato for sugguestions and assistance.

References

[1] Grochowski and R. Hoyt, "Future trends in hard disk drives", *IEEE Transactions on Magnetics*, vol.32, pp.1850-1854, May 1996.

[2] S. K. Aggarwal, D. A. Horsley, R. Horowitz, and A. P.Pisano, "Micro-actuators for High Density Disk Drives", in *Proceedings of the American Control Conference*, Albuquerque, New Mexico, pp.3979-3984, June, 1997.

[3] R.B. Evans, J.S. Griesbach and W.C. Messner, "Piezoelectric Microactuator for Dual Stage Control",*IEEE Transactions on Magnetics,* vol.35, pp.977-982, March 1999.

[4] S. Koganezawa, Y. Uematsu and T. Yamada, "Dual-Stage Actuator System for Magnet ic Disk Drives Using a Shear Mode Piezoelectric Microactuator",*IEEE Transactions on Magnetics,* vol.35, pp.988-992, March 1999.

[5] D. A. Horsley, N. Wongkomet,R. Horowitz, and A. P. Pisano, "Precision Positioning Using a Microfabricated Electrostatic Actuator",*IEEE Transactions on Magnetics,* vol.35, pp.993-999, March 1999.

[6] D. A. Horsley, D. Hernandez, R. Horowitz, A. K. Packard and A. P. Pisano, "Closed-Loop Control of a Microfabricated Actuator for Dual Stage Hard Disk Drive Servo Systems", in *Proceedings of the American Control Conference*, Philadelphia, PA, June, 1998.

[7] X. Hu, W. Guo, T. Huang and B. M.Chen, "Discrete time LQG/LTR Dual Stage Controller Deisgn and Implementation for High Tracking Density HDDS", in *Proceedings of the American Control Conference*, San Diego, CA, pp.4111-4115, June, 1999.

[8] D. Hernandez, S. S. Park, R. Horowitz, and A. K. Packard, "Dual-Stage Tracking-Following Servo Design for Hard Disk Drives", in *Proceedings of the American Control Conference*, San Diego, CA, pp.4116-4121, June, 1999.

[9] D.T. Phan "The Design and Modeling of Multirate Digital Control System for Disk Drive Applications", *Proceedings of the 1993 Asia-Pacific Workshop on Advances in motion control*,Singapore, pp.189-205,July 1993.

[10] T. Hara "Multi-rate Controller for Hard Disk Drive with Redesign of State Estimator", *Proceedings of the American Conference*, Philadephia, Pennsylvnia, June 1998.

[11] G.F. Franklin, J. Powell and M. Workman, *Digital Control of Dynamic Systems*, MA: Addison-Wesley, 2nd edition, 1990.

[12] A.V. Oppenheim and R.W. Schafer, *Discrete-Time Signal Processing*, Prentice Hall, 2nd edition,1998.

[13] R. Oboe, A. Beghi and B. Murari," Modeling and control of a dual stage actuator hard disk drive with piezoelectric secondary actuator", 1999 IEEE/ASME International Conference on Advanced Intelligent Mechatronics, , Atlanta, GA, pp.138-143, September 1999.

[14] T. Hirano, L.S. Fan, W. Y. Lee, J. Hong, W. Imaino, S. Pattanaik, S. Chan, P. Webb, R. Horowitz , S. Aggarwal and D. A. Horsley, "High-Bandwidth High-Accuracy Rotary Microactuators for Magnetic Hard Disk Drive Tracking Servos", *IEEE/ASME Transactions on Mechatronics*, vol.3, pp156-165, September 1998.

[15] S. J. Schroceck and W. C. Messner, "On Controller Design for Linear Time-Invariant Dual-Input Single-Output Systems", in *Proceedings of the American Control Conference*, San Diego, CA, pp.4122-4126, June 1999.

[16] K. Zhou, J.C. Doyle and K. Glover, *Robust and Optimal Control*, Prentice-Hall, Upper Saddle River, 1996.

[17] M. Kobayashi and R. Horowitz, "Track Seek Control for Hard Disk Drive Dual-Stage Servo Systems", in *Transaction on Magnetics*, Vol. 37, No. 2, March 2001.

[18] H. Numasato and M. Tomizuka, "Settling Control and Performance of Dual-Actuator System for Hard Disk Drives", in *Proceedings of the American Control Conference*, Arington, VA, pp.2779-2785, June 2001.

[19] T. Yamaguchi et., "Improvement of Settling Response of Disk Drive Head Positioning Servo using Mode Switching Control with Initial Value Compensation", in *Transaction on Magnetics*, Vol. 32, No. 3, May 1996.

[20] T. Yamguchi et, "Mode Switching Control Design with Initial Value Compensation and Its Application to Head Positioning Control on Magnetic Disk Drives", in *Transaction on Industrial Electronics*, Vol. 43, No.12, February 1996

[21] J. Ding, M. Tomizuka and H. Numasato, "Design and Robustness Analysis of Dual Stage Servo System"', in *Proceedings of the American Control Conference*, Chicago, IL, pp.2605-2609, June 2000.